Molecular Pharmacology Fast Forward. Published on February 18, 2016 as DOI: 10.1124/mol.115.102079
This article has not been copyedited and formatted. The final version may differ from this version.

Generation and Characterization of a Breast Cancer Resistance Protein Humanized Mouse Model

Shannon Dallas, Laurent Salphati, David Gomez-Zepeda, Thomas Wanek, Liangfu Chen, Xiaoyan Chu, Jeevan Kunta, Mario Mezler, Marie-Claude Menet, Stephanie Chasseigneaux, Xavier Declèves, Oliver Langer, Esaie Pierre, Karen DiLoreto, Carolin Hoft, Loic Laplanche, Jodie Pang, Tony Pereira, Clara Andonian, Damir Simic, Anja Rode, Jocelyn Yabut, Xiaolin Zhang and Nico Scheer

DMPK and Bioanalytical Research, Abbvie Deutschland GmbH & Co. KG, Ludwigshafen, Germany (MM, CH, LL).

Drug Metabolism and Pharmacokinetics, Genentech, Inc., 1 DNA Way, South San Francisco, CA 94080, USA (LS, JP, XZ)

Drug Metabolism and Pharmacokinetics, GlaxoSmithKline Pharmaceuticals, King of Prussia, Pennsylvania, USA (LC, CA, EP)

Health and Environment Department, AIT Austrian Institute of Technology GmbH, A-2444 Seibersdorf, Austria (TW, OL); Department of Clinical Pharmacology, Medical University of Vienna, Vienna, Austria (OL)

Preclinical Development & Safety, Janssen Research & Development, LLC, Spring House, PA, USA (SD, JK[1], KD, DS).

Merck Sharp & Dohme Corporation, Whitehouse Station, New Jersey, USA (XC, TP, JY)

Université Paris Descartes, UMR-S 1144, Paris, France (DGZ, MCM, SC, XD)

Taconic Biosciences GmbH, Neurather Ring 1, Koeln 51063, Germany (AR, NS); Current affiliation of AR and NS: Independent consultants, Cologne, Germany.

[1]Current affiliation: Discovery and Product Development, Teva Pharmaceuticals Research & Development, West Chester, PA, USA

Molecular Pharmacology Fast Forward. Published on February 18, 2016 as DOI: 10.1124/mol.115.102079
This article has not been copyedited and formatted. The final version may differ from this version.

Running title: BCRP humanized mice

Address correspondence to:

Laurent Salphati, Pharm.D., PhD, Department of Drug Metabolism and Pharmacokinetics, Genentech, Inc., 1 DNA Way, South San Francisco, CA 94080, USA.

Tel.: 650-467-1796; Fax: 650-467-3487; Email: salphati.laurent@gene.com

Number of text pages: 24

Number of Tables: 1

Number of Figures: 8

Number of references: 46

Number of words in Abstract: 250

Number of words in Introduction: 670

Number of words in Discussion: 1552

Nonstandard abbreviations used:

BBB, blood-brain barrier; BCRP, Breast cancer resistance protein; $Bcrp^{-/-}$, Bcrp knockout mice; %CV, coefficient of variation; DDI, drug-drug interactions; ES cells, embryonic stem cells; hBCRP, BCRP humanized mice; iv, intravenous; ITC, International Transporter Consortium; $K_{b,\ brain}$, brain-to-blood concentration ratio; PET, positron emission tomography; P-gp, P-glycoprotein; po, oral; qRT-PCR, quantitative reverse transcriptase PCR; WT, wild type.

Molecular Pharmacology Fast Forward. Published on February 18, 2016 as DOI: 10.1124/mol.115.102079
This article has not been copyedited and formatted. The final version may differ from this version.

Abstract

The breast cancer resistance protein (BCRP) is expressed in various tissues, such as the gut, liver, kidney and blood brain barrier (BBB), where it mediates the unidirectional transport of substrates to the apical/luminal side of polarized cells. Thereby BCRP acts as an efflux pump, mediating the elimination or restricting the entry of endogenous compounds or xenobiotics into tissues and it plays important roles in drug disposition, efficacy and safety. Bcrp knockout mice ($Bcrp^{-/-}$) have been used widely to study the role of this transporter in limiting intestinal absorption and brain penetration of substrate compounds. Here we describe the first generation and characterization of a mouse line humanized for BCRP (hBCRP), in which the mouse coding sequence from the start to stop codon was replaced with the corresponding human genomic region, such that the human transporter is expressed under control of the murine *Bcrp* promoter. We demonstrate robust human and loss of mouse BCRP/Bcrp mRNA and protein expression in the hBCRP mice and the absence of major compensatory changes in the expression of other genes involved in drug metabolism and disposition. Pharmacokinetic and brain distribution studies with several BCRP probe substrates confirmed the functional activity of the human transporter in these mice. Furthermore, we provide practical examples for the use of hBCRP mice to study drug-drug interactions (DDIs). The hBCRP mouse is a promising model to study the in vivo role of human BCRP in limiting absorption and BBB penetration of substrate compounds and to investigate clinically relevant DDIs involving BCRP.

Molecular Pharmacology Fast Forward. Published on February 18, 2016 as DOI: 10.1124/mol.115.102079
This article has not been copyedited and formatted. The final version may differ from this version.

Introduction

BCRP, also referred to as ABCG2, is a member of the superfamily of ATP-binding-cassette (ABC) transporters, some of which have important roles in the transport of various drugs and their metabolites (Chan et al., 2004; Leslie et al., 2005). BCRP is expressed in many different cell types, such as the luminal membrane of enterocytes, the canalicular membrane of hepatocytes, kidney proximal tubule epithelia, the luminal side of the microvascular brain endothelial cells composing the BBB, and the placenta, where it mediates the elimination and can restrict the entry of compounds into tissues (Meyer zu Schwabedissen and Kroemer, 2011). BCRP has attracted attention in drug discovery and development because of its ability to transport many commonly prescribed drugs, such as anticancer agents (e.g. topotecan, doxorubicin, methotrexate, imatinib, sorafenib or mitoxantrone), the HMG-CoA reductase inhibitor rosuvastatin, the anti-inflammatory drug sulfasalazine, the sympatholytic drug prazosin and many others (Ni et al., 2010). Furthermore, several BCRP inhibitors, such as ritonavir, omeprazole, imatinib, ivermectin, and curcumin, have been described (Jani et al., 2011; Kusuhara et al., 2012; Ni et al., 2010). Inhibition of BCRP and polymorphic variations associated with altered BCRP activity were shown to result in pharmacokinetic changes of BCRP substrates in the clinic (Hua et al., 2012; Kusuhara et al., 2012; Urquhart et al., 2008; Yamasaki et al., 2008; Zhang et al., 2006). Based on its clinical relevance, the International Transporter Consortium (ITC), followed by the FDA and EMA regulators, has recommended BCRP as one of the key transporters to be evaluated for substrate and inhibitor interactions during drug development (Giacomini et al., 2010; Zamek-Gliszczynski et al., 2012b).

Such interactions of BCRP with substrates and inhibitors are routinely tested in vitro using overexpression systems or whole cells and, theoretically, physiologically-based pharmacokinetic modelling approaches can then help to further predict complex DDIs (Rostami-Hodjegan, 2012). Despite the great value of these technologies, predicting the

Molecular Pharmacology Fast Forward. Published on February 18, 2016 as DOI: 10.1124/mol.115.102079
This article has not been copyedited and formatted. The final version may differ from this version.

effects of transporters on human pharmacokinetics and DDI potential from in vitro data alone remains challenging and preclinical in vivo studies can provide useful complementary information in this regard. Bcrp knockout mice (Jonker et al., 2002) and, more recently, rats (Zamek-Gliszczynski et al., 2012a) have helped to determine the impact of Bcrp on the pharmacokinetics and tissue distribution of various substrates, including sulfasalazine (Zaher et al., 2006; Zamek-Gliszczynski et al., 2012a), topotecan (de Vries et al., 2007), rosuvastatin (Kitamura et al., 2008), sorafenib (Lagas et al., 2010), daidzein and genistein (Enokizono et al., 2007).

However, species differences associated with this transporter may limit the use of these knockout models in predicting the role of BCRP in humans (Chu et al., 2013). While most investigations have focused on the differences in the BCRP expression level between animals and man (Chu et al., 2013; Lai, 2009; Li et al., 2009; Uchida et al., 2011; Warren et al., 2009), a few studies have also reported species differences in BCRP substrate specificity or interaction with inhibitors (Gonzalez-Lobato et al., 2010; Li et al., 2008; Mazur et al., 2012). Although the amino-acid sequences between mouse Bcrp and human BCRP are 81% identical and 86% homologous and therefore relatively conserved (Doyle and Ross, 2003), these proteins vary in more than 90 amino acids. As a single amino acid polymorphism in human BCRP can significantly alter its transport efficiency compared to the WT protein (Lee et al., 2007; Urquhart et al., 2008), differences in the kinetics of BCRP-mediated drug transport between human and mouse are very likely. Accordingly, in order to study the in vivo role of the human instead of the mouse transporter under preclinical conditions, a BCRP humanized mouse model would be of great value.

In the present work we describe the generation and extensive characterization of such a hBCRP mouse model, expressing the human in lieu of the mouse transporter under control of the murine Bcrp promoter. We determined the mRNA and protein expression, evaluated

Molecular Pharmacology Fast Forward. Published on February 18, 2016 as DOI: 10.1124/mol.115.102079
This article has not been copyedited and formatted. The final version may differ from this version.

potential compensatory changes in the expression of other genes involved in drug disposition, assessed functional activity of BCRP and conducted proof-of-concept studies for using the hBCRP mice for DDI assessment.

Molecular Pharmacology Fast Forward. Published on February 18, 2016 as DOI: 10.1124/mol.115.102079
This article has not been copyedited and formatted. The final version may differ from this version.

Materials and Methods

Chemicals and Reagents. Ultra-High Performance Liquid Chromatography (UHPLC) tandem mass spectrometry (MS/MS) protein quantification: HBSS, HEPES, Tris-HCl and sodium phosphate (Na_2HPO_4 and NaH_2PO_4) were acquired from Sigma Aldrich (Saint Quentin Fallavier, France). Reagents used for plasma membrane isolation and protein digestion, NaCl, $MgCl_2$, KCl, sucrose, EDTA, Guanidine-HCl, DTT, iodoacetamide, bovine serum albumin (BSA), dextran (molecular weight 70.000) and urea also came from Sigma Aldrich (Saint Quentin Fallavier, France). The complete Mini (EDTA-free) Protease Inhibitor Cocktail tablets were purchased from Roche (Bâle, Switzerland). Chloroform (HiPerSolv, Chromanorm for HPLC) was supplied by VWR (Strasbourg, France). HPLC-grade acetonitrile and methanol were purchased at Merck (Nogent-sur-Marne, France). Formic acid (99% w/w), HPLC grade, was supplied by Fischer Scientific (Illkirch, France). All the water was prepared with a Milli-Q water purification system (Millipore, Molsheim, France). Sequencing grade Modified Trypsin, Mass Spectrometry grade rLys-C and ProteaseMAX surfactant were from Promega (Charbonnières-les-Bains, France). The measurement of protein concentration was carried out by using the Micro BCA Protein Assay Kit (Thermo Scientific, Illkirch, France). Standard solutions of peptides were provided by Pr. M. Vidal and Dr. W. Q. Liu (UMR 8638, Chimie organique médicinale et extractive - Toxicologie expérimentale) or by Pepscan (Lelystad, The Netherlands). The accurate concentration of each standard solution was determined, after acid hydrolysis and amino-acid analysis by Dr. E. Thioulouse (Laboratoire de Biochimie, Hôpital Trousseau, Paris, France) or by Pepscan (Lelystad, The Netherlands).

Sulfasalazine/Ko143 interaction, daidzein, genistein, rosuvastatin and topotecan in vivo studies: Sulfazalasine, daidzein, genistein and topotecan were purchased from Sigma-Aldrich (St. Louis, MO) and Ko143 from Enzo Life Sciences (Plymouth Meeting, PA). Rosuvastatin

Molecular Pharmacology Fast Forward. Published on February 18, 2016 as DOI: 10.1124/mol.115.102079
This article has not been copyedited and formatted. The final version may differ from this version.

was obtained from TSZ Chem (Framingham, MA). 1-methyl-2-pyrrolidone (NMP), Solutol (Kolliphor HS 15), thenyoltrifluoroacetone (TTFA), DMSO and Tween20 were obtained from Sigma-Alrich (St. Louis, MO). Saline was obtained from Baxter (Deerfield, IL). Ammonium acetate and glacial acetic acid were obtained from Fisher Scientific (Waltham, MA).

Positron emission tomography (PET) study: Tariquidar dimesylate and Ko143 for the PET study were obtained from Xenova Ltd. (Slough, UK) and Axon Medchem BV (Groningen, The Netherlands), respectively.

Generation of hBCRP and Bcrp$^{-/-}$ mice. hBCRP and Bcrp$^{-/-}$ mice were generated by Taconic Biosciences GmbH (Cologne, Germany) as described below. DNA constructs and cloning: For targeting the *Bcrp* gene locus basic vectors containing (1) neomycin and puromycin expression cassettes flanked by *frt* and *f3* sites, respectively, (2) a ~5 kb genomic sequence upstream of the translational start ATG of the mouse *Bcrp* gene on exon 2 and a ~7 kb genomic sequence downstream of the stop codon on exon 16 used as targeting arms for homologous recombination have been constructed. The final targeting vector shown in Fig. 1B was generated by fusing a genomic fragment from start ATG to stop codon of human *BCRP* in frame to the aforementioned targeting arms by subcloning the fragments via consecutive red/ET recombineering (Zhang et al., 1998) into the bacterial artificial chromosome RP11-183N11 (Source BioScience, Nottingham, United Kingdom) containing the genomic sequence of human *BCRP*. The coding exons 2-16 from this clone were sequences and confirmed to match the human BCRP reference sequence (http://www.uniprot.org/uniprot/Q9UNQ0).

Generation and molecular characterization of targeted embryonic stem cells: Culture and targeted mutagenesis of embryonic stem (ES cells) were carried out as described previously (Behringer et al., 2014). The targeting vector was linearized with *Not*I and electroporated into a C57BL/6NTac mouse ES cell line. Of 256 G418 and puromycin resistant ES cell colonies screened by standard Southern blot analyses, 14 correctly targeted clones were identified, 4 of

Molecular Pharmacology Fast Forward. Published on February 18, 2016 as DOI: 10.1124/mol.115.102079
This article has not been copyedited and formatted. The final version may differ from this version.

which were expanded and further analysed by Southern blot analyses with 5' and 3' external probes and internal probes. All of these clones were confirmed as correctly targeted at both homology arms without additional random integrations (data not shown).

Generation and molecular characterization of hBCRP and Bcrp$^{-/-}$ mice: For the generation of hBCRP mice, 3 correctly targeted ES cell clones were expanded, injected into BALBc-blastocysts and transferred into foster mothers as described previously (Behringer et al., 2014). Litters from these fosters were inspected visually and chimerism was determined by hair colour. Highly chimeric animals obtained from one of the 3 correctly targeted clones were used for breeding to an efficient flipase (Flpe) deleter strain carrying a transgene that expresses Flpe in the germ line in order to delete the neomycin and puromycin expression cassettes in the offspring (Fig. 1D). Offspring from these crosses were analysed by PCR in order to identify heterozygous *BCRP* humanized mice. These heterozygous mice were either crossed with each other to generate homozygous hBCRP mice or crossed to a deleter strain carrying a transgene that expresses Cre-recombinase in the germ line in order to delete the human *BCRP* exons 3-15 (Fig. 1E). Offspring from the latter crosses were analysed by PCR in order to identify heterozygous *Bcrp* knockout mice, which were then further crossed to generate homozygous Bcrp$^{-/-}$ mice. The Flpe- and Cre-deleter strains mentioned above were generated in house on a C57BL/6NTac genetic background.

Animal husbandry and experimentation. hBCRP and Bcrp$^{-/-}$ mice were bred at Taconic Biosciences GmbH (Cologne, Germany) to obtain homozygous age-matched mice and age- and sex-matched C57BL/6NTac wild type (WT) controls were obtained from Taconic Biosciences, Inc. (Hudson, NY). These three mouse lines are maintained and available through Taconic Biosciences. Animals were allowed to acclimatize for at least five days prior to an experimental procedure at all experimental locations. Mice were kept in agreement with local laws and regulations and in temperature-controlled environments with 12-hour light cycles and given standard diets and water ad libitum. All animal procedures were approved by

Molecular Pharmacology Fast Forward. Published on February 18, 2016 as DOI: 10.1124/mol.115.102079
This article has not been copyedited and formatted. The final version may differ from this version.

local Institutional Animal Care and Use Committees.

Quantitative Reverse Transcriptase PCR (qRT-PCR). Details on the preparation of mRNA, the synthesis of cDNA, the primers used and the methods of data analysis for qRT-PCR are provided in the Supplemental Materials and Methods.

Affymetrix expression profiling (Microarray Analysis). Details on the preparation of mRNA, quality and quantity determination, cDNA synthesis, used GeneChip Array and data processing methods are provided in the Supplemental Materials and Methods.

Cortical microvessel isolation, preparation of plasma membrane fraction from different tissues, protein digestion and quantification by UHPLC MS/MS. Details on the isolation of brain microvessels, preparation of plasma membrane fraction from microvessels, liver and kidney, protein digestion and quantification by UHPLC MS/MS are provided in the Supplemental Materials and Methods.

Sulfasalazine, daidzein, genistein, rosuvastatin and topotecan in vivo studies. Details on the sulfasalazine, daidzein. genistein, rosuvastatin and topotecan pharmacokinetics studies and the sulfasalazine/Ko143 interaction study and corresponding LC-MS/MS and pharmacokinetic analyses are provided in the Supplemental Materials and Methods.

PET study. Details on general procedures, animal handling, PET imaging, metabolite analysis and statistical analysis are provided in the Supplemental Materials and Methods.

Statistical analysis. Student's t-test or one-way ANOVA were applied to determine statistical significances in differences between WT, Bcrp$^{-/-}$ and hBCRP mice. Values were considered statistically different when $p<0.05$. Analyses were done using Microsoft Excel or GraphPad Prism 5.

Molecular Pharmacology Fast Forward. Published on February 18, 2016 as DOI: 10.1124/mol.115.102079
This article has not been copyedited and formatted. The final version may differ from this version.

Results

Generation of hBCRP and Bcrp$^{-/-}$ mice. hBCRP mice were generated by a knock-in strategy as depicted in Fig. 1, such that the coding sequence of mouse Bcrp from its start codon on exon 2 to its stop codon on exon 16 was replaced by the corresponding genomic human region in mouse ES cells (Fig. 1A-D). As a result of this approach the human instead of mouse transporter is expressed under control of the mouse Bcrp promoter. Transgenic mice were generated from correctly targeted ES cells. The neomycin and puromycin expression cassettes used for ES cell clone selection were deleted via Flp-recombinase mediated recombination in vivo by crossing hBCRP transgenic mice with a mouse line expressing Flp-recombinase in the germ line (Fig. 1D). Functional inactivation of the BCRP gene was achieved by crossing hBCRP mice with a mouse line expressing Cre-recombinase in the germ line resulting in a deletion of human BCRP exons 3-15 (Fig. 1E). Homozygous hBCRP and Bcrp$^{-/-}$ mice obtained by breeding appeared normal, could not be distinguished from WT animals, and had normal survival rates and fertility.

Human *BCRP* and mouse *Bcrp* mRNA expression in WT, hBCRP and Bcrp$^{-/-}$ mice. In order to confirm expression of human *BCRP* mRNA in different tissues of the hBCRP mice, a TaqMan analysis was conducted on liver, kidney, duodenum, ileum, jejunum, colon, heart, lung, testis and whole brain samples of WT, hBCRP and Bcrp$^{-/-}$ male and female mice, using a mouse Bcrp and a human BCRP specific TaqMan assay (n=3 mice per sex and genotype). The human *BCRP* mRNA was detectable in all tissues of the hBCRP mice, but not in WT or Bcrp$^{-/-}$ animals. Based on Ct values the highest expression was observed in the kidney, followed by ileum, duodenum and jejunum, colon, testis, liver, brain, lung and heart (Supplemental Table 1). The same pattern of expression was observed for mouse *Bcrp* in WT mice, when a murine specific *Bcrp* TaqMan assay was used (Supplemental Table 1). Compared to murine *Bcrp* mRNA in WT animals, human *BCRP* in the hBCRP mice was

Molecular Pharmacology Fast Forward. Published on February 18, 2016 as DOI: 10.1124/mol.115.102079
This article has not been copyedited and formatted. The final version may differ from this version.

expressed at slightly lower levels, with some variability between organs. While the *Bcrp*/*BCRP* expression in the brain was almost identical between WT and hBCRP mice, the human *BCRP* expression in the kidney and the testis of the hBCRP mice was only ~30% of the murine *Bcrp* expression in the WT. All other values varied between these two extremes (Fig. 2). In general the expression level of mouse *Bcrp* in WT animals was similar between both sexes for most organs, except in the liver where it was 2.5-fold lower and in the duodenum and ileum where it as ~1.5-fold higher in females compared to males. The hBCRP mice showed the same difference in human *BCRP* expression between males and females for the liver and the ileum, while the level was identical between both sexes in the duodenum (Fig. 2, Supplemental Table 1). In summary, a robust expression of human *BCRP* mRNA in absence of mouse *Bcrp* mRNA expression was observed in hBCRP mice. The differences in relative expression levels between organs were the same as that of mouse *Bcrp* in WT mice with similar variations between males and females, albeit the human transcript was expressed at slightly lower levels than its mouse orthologue.

Bcrp/BCRP protein quantification in WT and hBCRP mice. Bcrp/BCRP protein amounts in WT and hBCRP mice were determined in kidney (n=3 mice per strain), liver (n=3 mice per strain) and cortical brain vessels (n=2 mice for WT and n=3 mice for hBCRP) by UHPLC MS/MS analysis using peptides specific to human BCRP, or to mouse Bcrp, and additionally peptides that are in common to both mouse and human Bcrp/BCRP (Supplemental Table 2). The plasma membrane marker Na^+/K^+ ATPase was used as a control to evaluate the extraction and digestion homogeneity between each tissue samples, as previously proposed (Hoshi et al., 2013). The homogeneity of liver and kidney samples was confirmed by the low variability of Na^+/K^+ ATPase amounts with coefficients of variation (%CV) of 8.9 and 24.9% in WT mice and 8.6 and 13.6% in hBCRP mice, respectively (Table 1). Cortical vessels were less homogenous due to the low protein amounts available for the assay of each sample (%CV

Molecular Pharmacology Fast Forward. Published on February 18, 2016 as DOI: 10.1124/mol.115.102079
This article has not been copyedited and formatted. The final version may differ from this version.

= 31.9% in WT and 32.9% in hBCRP mice). No significant differences in Na^+/K^+ ATPase expression levels were observed in any sample between WT and hBCRP mice (Table 1).

The peptide specific to human BCRP was detected in all samples of hBCRP but not WT mice, while the opposite was the case for the mouse Bcrp-specific peptide (data not shown). For direct comparison of protein amounts between WT and hBCRP mice we used the data obtained with the common Bcrp/BCRP peptide (Table 1). Consistent with the mRNA analysis, the highest Bcrp/BCRP protein expression was observed in kidney (WT = 37.7, hBCRP = 9.34 fmol/µg of protein), followed by liver (WT = 1.55, hBCRP = 0.73 fmol/µg of protein) and brain cortical vessels (WT = 0.23, hBCRP = 0.39 fmol/µg of protein). The average Bcrp/BCRP protein amount in hBCRP mice was 4-fold lower in kidney ($p < 0.001$), 2.1-fold lower in liver ($p < 0.001$) and 1.7-fold higher in brain vessels (statistically not significant) compared to WT controls, which overall is in reasonable agreement with the mRNA measurements.

Assessment of hepatic gene expression changes in Bcrp$^{-/-}$ and hBCRP mice. Potential compensatory gene expression changes in liver of Bcrp$^{-/-}$ and hBCRP mice relative to WT controls were assessed by microarray analysis. The comparison between Bcrp$^{-/-}$ and WT mice revealed a total of 22 unique genes (24 total, including genes that are duplicated within the array) altered by greater than 2-fold ($p < 0.05$) (Supplemental Table 3). As expected, the hepatic expression of mouse *Bcrp* was most significantly suppressed compared to WT controls (87-fold decrease). Other expression changes in genes coding for proteins (potentially) involved in drug metabolism and disposition were observed for monooxygenase DBH-like (*Moxd*) 1 (17.6-fold increase in Bcrp$^{-/-}$ compared to WT mice), solute carrier 3a1 and 41a2 (2.1 and 2.0-fold increase, respectively) and the cytochrome P450 isoform 2b10 (3-fold decrease). In addition, significant changes were noted in some genes not involved in drug metabolism and disposition, such as lipocalin 2, orosomucoid 2 (which can be involved in

Molecular Pharmacology Fast Forward. Published on February 18, 2016 as DOI: 10.1124/mol.115.102079
This article has not been copyedited and formatted. The final version may differ from this version.

plasma protein binding of certain drugs (Silamut et al., 1991)), metallothionein 2, and serum amyloid A3 (8.6, 4.9. 4.7 and 4.2-fold increase, respectively). Relative comparison of hBCRP to WT mice detected 4 genes as significantly changed. In addition to the 78-fold decrease of hepatic *Bcrp*, an 8.7-fold increase of *Moxd1* expression was the only change of genes coding for proteins involved in drug metabolism and disposition. Additionally, serpine 2 was increased by 2.6-fold and the transmembrane protein 223 was decreased by 2.6-fold (Supplemental Table 3).

Concentration of sulfasalazine, daidzein, genistein, rosuvastatin and topotecan in blood and other tissues of WT, hBCRP and Bcrp$^{-/-}$ mice. The expression of functional BCRP in hBCRP mice was assessed by comparing the concentration-time profiles of various BCRP probe substrates in blood and different tissues of WT, hBCRP and Bcrp$^{-/-}$ mice.

Sulfasalazine: Following 5 mg/kg intravenous (iv) or 20 mg/kg oral (po) administration of sulfasalazine, blood concentrations were markedly higher in Bcrp$^{-/-}$ than in WT and hBCRP mice (Fig. 3A and B). In WT mice, blood concentrations were below the limit of quantitation after 2 and 1 hour, for the iv and po dose, respectively. Consequently, PK analyses and comparisons of WT animals with the two other strains were performed with parameters calculated using concentrations up to 1 or 2 hours (Supplemental Table 4A), as well as based on the complete profiles (up to 6 hours; Supplemental Table 4B) from the other strains.

Blood exposure to sulfasalazine was significantly ($p<0.05$) increased in Bcrp$^{-/-}$ compared to WT mice after iv (8.3-fold) and po (117-fold) administration (Supplemental Table 4A). Concentrations (and profiles) in hBCRP mice were intermediate between those observed in the WT and Bcrp$^{-/-}$ mice (Figs. 3A and B), with concentrations measurable up to 6 hours. This was reflected by a modest 2.7- fold higher AUC_{0-2} in humanized compared to WT mice following iv dosing and 4.6- fold higher AUC_{0-1} after po administration. Importantly, sulfasalazine exposure in hBCRP mice was nevertheless significantly ($p<0.05$) lower than in

Molecular Pharmacology Fast Forward. Published on February 18, 2016 as DOI: 10.1124/mol.115.102079
This article has not been copyedited and formatted. The final version may differ from this version.

Bcrp$^{-/-}$ animals (Supplemental Tables 4A and B) after dosing through either route. Clearance in Bcrp$^{-/-}$ mice was 8.4-fold lower than in WT controls, while in hBCRP mice, it was only decreased by 2.7-fold.

Daidzein: The plasma concentration of daidzein was slightly increased in Bcrp$^{-/-}$ compared to WT mice over a period of one hour after administration of a 5 mg/kg iv dose, with a significant 1.5-fold higher plasma concentration at the earliest measured time point (5 minutes after administration). In contrast, the concentration-time profiles in hBCRP and WT mice were comparable (Fig. 4A, B). The mean brain concentrations of daidzein were significantly higher in Bcrp$^{-/-}$ compared to WT mice at 0.5, 1 and 2 hrs after administration, but comparable between WT and hBCRP animals (Figure 4C-E). Namely, at the 0.5 hrs time point the daidzein mean brain concentration was increased by ~4.7-fold in Bcrp$^{-/-}$ compared to WT and hBCRP mice (Fig. 4C). This difference is also reflected by the significantly higher brain-to-plasma concentration ratio in Bcrp$^{-/-}$ mice (1.13) relative to WT (0.20) and hBCRP (0.11) animals. At the 1 and 2 hr time points daidzein was below the limit of quantification in brain tissue of WT and hBCRP mice, but still detectable in Bcrp$^{-/-}$ mice (Fig. 4D and E).

Genistein: The blood concentration of genistein was higher in Bcrp$^{-/-}$ compared to WT mice (Fig. 5A-C), with statistically significant 2.2- and 2.2-fold increases in $AUC_{0\text{-}24hrs}$ following 20 mg/kg iv and 50 mg/kg po administration, respectively (Supplemental Table 5). Furthermore, the $AUC_{0\text{-}6hrs}$ was 2.0-fold higher in Bcrp$^{-/-}$ mice receiving a 20 mg/kg po dose of genistein, while the blood clearance in these mice after 20 mg/kg iv administration was 2.4-fold lower relative to the WT controls (Supplemental Table 5). The Bcrp$^{-/-}$ animals also showed a statistically significant 1.5-fold higher $AUC_{0\text{-}6hrs}$ and $AUC_{0\text{-}24hrs}$ following 20 and 50 mg/kg po doses of genistein compared to hBCRP mice (Supplemental Table 5). Brain concentrations were analysed 15 and 90 min after 20 mg/kg iv administration of genistein. Bcrp$^{-/-}$ mice showed significantly higher brain concentrations than WT and hBCRP animals at both time points, with 2.6 and 4.4-fold increases at 15 min and 8.1 and 9.9-fold increases at

Molecular Pharmacology Fast Forward. Published on February 18, 2016 as DOI: 10.1124/mol.115.102079
This article has not been copyedited and formatted. The final version may differ from this version.

90 min compared to WT and hBCRP mice, respectively (Fig. 5D and E). Furthermore, the brain-to-blood concentration ratio ($K_{b,\ brain}$) values in Bcrp$^{-/-}$ mice were 3.3 and 5.1-fold higher at 15 min and 19.0 and 7.6-fold higher at 90 min than in WT and hBCRP animals (Fig. 5F). Genistein concentrations were also measured in testis, liver and kidney following 20 mg/kg iv administration, but most differences between WT, Bcrp$^{-/-}$ and hBCRP mice were not significant (data not shown).

Rosuvastatin: Bcrp$^{-/-}$ mice showed statistically significant higher blood concentrations of rosuvastatin compared to WT controls following 6.1 mg/kg iv and 13.7 mg/kg po administration (Fig. 6A, B), as reflected by 4.2 and 3.1-fold $AUC_{0\text{-}24hrs}$ and 1.7 and 6.7-fold increases in C_{max} at these doses, respectively (Supplemental Table 6). In contrast, hBCRP mice showed no statistically significant difference in rosuvastatin blood concentrations to WT animals after iv administration and only marginal and statistically insignificant 1.6 and 1.7-fold increases in $AUC_{0\text{-}24hrs}$ and C_{max} following oral administration (Fig. 6A, B, Supplemental Table 6). Brain, kidney and liver concentrations were also measured at 15 min and 1 h after po administration, but due to the small number of animals and high variability between individual mice from each group no significant changes were observed between the different lines (data not shown). The % recovery of parent compound in feces and urine after iv administration and in urine after oral administration of rosuvastatin was highest in WT and lowest in Bcrp$^{-/-}$ mice, with hBCRP animals in between (Supplemental Table 7).

Topotecan: Following 1 mg/kg iv and po administration the topotecan blood concentrations in Bcrp$^{-/-}$ mice were higher compared to WT controls (Fig. 7A and B), with concomitant significant 6.1-fold increases in $AUC_{0\text{-}4h}$ after po dosing (Supplemental Table 8). Blood concentrations in hBCRP mice were between these two lines (Fig. 7A and B), showing a significant 1.5-fold lower $AUC_{0\text{-}4h}$ than Bcrp$^{-/-}$ mice after po administration (Supplemental Table 8). Compared to WT animals the clearance after iv administration was 1.6 and 1.4-fold lower in Bcrp$^{-/-}$ and hBCRP mice, respectively. Following po administration the C_{max} in Bcrp^{-}

Molecular Pharmacology Fast Forward. Published on February 18, 2016 as DOI: 10.1124/mol.115.102079
This article has not been copyedited and formatted. The final version may differ from this version.

$^{/-}$ mice was increased by 5.6 and 1.7-fold relative to WT and hBCRP animals, respectively (Supplemental Table 8). While no significant differences were observed between the three lines in topotecan brain exposure 15 minutes after 1 mg/kg po administration (Fig. 7C), brain concentrations were moderately, but statistically significantly increased by 3.1 and 1.7-fold after 60 minutes in Bcrp$^{-/-}$ mice compared to WT and hBCRP animals, respectively (Fig. 7D). As a consequence of the lower topotecan blood concentrations in WT mice, $K_{b,\ brain}$ values were higher relative to Bcrp$^{-/-}$ and hBCRP mice at both time points (Fig. 7E).

BCRP inhibition studies related to oral bioavailability of sulfasalazine and brain penetration of tariquidar. The possibility of inhibiting intestinal BCRP activity was tested by treating WT, Bcrp$^{-/-}$ and hBCRP mice with a 20 mg/kg po dose of Ko143 30 minutes prior to the administration of 20 mg/kg po sulfasalazine. No significant changes in sulfasalazine blood concentrations, $AUC_{0\text{-last}}$ and C_{max} were observed in Ko143 pre-treated relative to untreated Bcrp$^{-/-}$ mice (Fig. 3C, Supplemental Table 4B). In contrast, pre-treatment with Ko143 increased the blood concentrations of sulfasalazine in WT and hBCRP mice (Fig. 3C), detectable up to 6 hours post-dose. This was associated with significant 25.8 and 6.5-fold increases in $AUC_{0\text{-}1}$ and 45.6 and 5.3-fold increases in $AUC_{0\text{-last}}$ in WT and hBCRP mice, respectively (Supplemental Table 4A and B). Although C_{max} in WT mice under control conditions could only be estimated from three timepoints, it was significantly increased from 0.25 µM to 5.36 µM with Ko143. Similarly, C_{max} in hBCRP mice was 5-2-fold greater in the presence of Ko143 (Supplemental Table 4B).

We also assessed the functional activity of BCRP/Bcrp and its inhibition at the BBB of hBCRP and WT mice in vivo using positron emission tomography (PET) and [^{11}C]tariquidar as radiotracer, which is a metabolically stable substrate of murine and human P-glycoprotein (P-gp) as well as murine Bcrp and human BCRP (Bankstahl et al., 2013; Kannan et al., 2011). We have shown before that [^{11}C]tariquidar can be used to visualize Bcrp functional activity at the murine BBB when used at P-gp-saturating tariquidar plasma concentration levels (Wanek

Molecular Pharmacology Fast Forward. Published on February 18, 2016 as DOI: 10.1124/mol.115.102079
This article has not been copyedited and formatted. The final version may differ from this version.

et al., 2012). Mice underwent [^{11}C]tariquidar PET scans after (i) pretreatment with vehicle only, (ii) pretreatment with unlabelled tariquidar at a dose of 12 mg/kg which inhibits P-gp at the BBB without inhibiting BCRP/Bcrp and (iii) pretreatment with tariquidar (12 mg/kg) and the BCRP/Bcrp inhibitor Ko143 (10 mg/kg) (Allen et al., 2002) as described previously (Wanek et al., 2012) (Fig. 8). We assessed radiolabelled metabolites of [^{11}C]tariquidar in plasma and brain samples collected at the end of PET scanning by radio-TLC analysis. At 60 minutes after [^{11}C]tariquidar injection 80 ± 14% (n = 12) and 85 ± 12% (n = 11) of radioactivity in plasma and 93 ± 8% (n = 6) and 97 ± 2% (n = 3) in brain was in the form of unchanged [^{11}C]tariquidar for hBCRP and WT mice, respectively. This suggested that there were no differences in radiotracer metabolism between hBCRP and WT mice. Brain uptake of [^{11}C]tariquidar was expressed as $K_{b,brain}$ of radioactivity in the last PET frame (i.e. at 50-60 minutes after radiotracer injection). In vehicle scans, $K_{b,brain}$ values were low and not significantly different between hBCRP and WT mice ($K_{b,brain}$ (mean ± SD) hBCRP: 1.58 ± 0.38; WT: 1.50 ± 0.25), which was consistent with restriction of brain distribution of [^{11}C]tariquidar by P-gp and BCRP/Bcrp. In scans after P-gp inhibition with tariquidar (12 mg/kg), $K_{b,brain}$ values were only moderately and not significantly increased as compared with vehicle treated animals in hBCRP mice ($K_{b,brain}$: 3.20 ± 0.21, 2.0-fold increase) and WT mice ($K_{b,brain}$: 3.35 ± 0.31, 2.2-fold increase), which was consistent with functional compensation of P-gp inhibition by BCRP/Bcrp for dual P-gp/BCRP substrates (Kodaira et al., 2010). In scans after P-gp and BCRP/Bcrp inhibition with tariquidar (12 mg/kg) and Ko143 (10 mg/kg), respectively, $K_{b,brain}$ values were significantly (P<0.001, 1-way ANOVA followed by Bonferroni´s multiple comparison test) increased as compared with tariquidar only treated animals by 3.6-fold in hBCRP mice ($K_{b,brain}$: 11.66 ± 2.16) and by 3.3-fold in WT mice ($K_{b,brain}$: 10.90 ± 0.93). This strongly suggested that hBCRP and WT mice had comparable functional activity of BCRP/Bcrp at the BBB and that this transporter was effectively inhibited by Ko143.

Molecular Pharmacology Fast Forward. Published on February 18, 2016 as DOI: 10.1124/mol.115.102079
This article has not been copyedited and formatted. The final version may differ from this version.

Discussion

Here, we describe the generation of a humanized BCRP mouse model via a sophisticated replacement of the murine *Bcrp* coding sequence with corresponding human genomic DNA, such that the human transporter is expressed under control of the mouse *Bcrp* promoter (Fig. 1). The hBCRP mice were healthy and showed no obvious phenotypic abnormalities. Human *BCRP* mRNA was detected in the expected organs, such as liver, gut, brain, kidney and testis of humanized mice, albeit at slightly lower levels than mouse *Bcrp* mRNA in WT mice in most tissues (Fig. 2). The mRNA measurement were further confirmed by protein quantification in selected organs, showing the BCRP amounts to be 2 and 4-fold lower in liver and kidney, respectively, and 1.7-fold higher (not statistically significant) in cortical vessels of hBCRP compared to WT mice (Table 1).

Although the hepatic and renal protein amounts of Bcrp and Na^+/K^+ ATPase in membrane fractions are within the same magnitude as previously reported by Kamiie et al. using similar extraction methods on tissues from a ddy WT mouse strain (Kamiie et al., 2008), we observed lower Bcrp levels in the C57BL/6NTac mice used in our study (1.55 vs 8.84 fmol/µg of protein). The most likely explanation for this is an inter-strain difference. When comparing our results for cortical vessels with those previously described in C57BL/6 mice by Sadiq et al. (Sadiq et al., 2015), we measured significantly lower levels in this tissue (0.225 fmol/µg vs 8.69 fmol/µg of protein). However, the method of vessel isolation differed between the two studies, such that Sadiq et al. obtained capillaries from whole brain lysate and carried out three successive filtrations (210, 85 and 20 µm nylon mesh) in order to enrich in microcapillaires, whereas we used only one 10 µm nylon mesh to filter cortical vessels. Therefore, the lower values can be explained by a dilution of Bcrp/BCRP in our samples. Taking into account that the average BCRP/Bcrp protein amount in the human BBB was

Molecular Pharmacology Fast Forward. Published on February 18, 2016 as DOI: 10.1124/mol.115.102079
This article has not been copyedited and formatted. The final version may differ from this version.

recently shown to be 1.85-fold greater than in WT mice (Uchida et al., 2011) and that we observed a 1.75-fold higher expression level of human BCRP in cortical vessels of hBCRP mice than murine Bcrp in WT controls (Table 1), we conclude that the expression level of this transporter in hBCRP mice and humans is similar. The comparison of BCRP protein levels between humans and hBCRP mice in other organs requires further investigation.

No compensatory changes in the expression of genes coding for proteins involved in drug metabolism and disposition were observed in liver of hBCRP mice compared to WT controls with the exception of an 8.7-fold increase of *Moxd1* mRNA (Supplemental Table 3). The presumably very minor role of Moxd1 in drug metabolism and disposition (Chambers et al., 1998) and the moderate (2.6-fold) change of only two other genes, serpine 2 and transmembrane protein 223, in hBCRP mice, are not expected to limit their use to study BCRP-mediated absorption or disposition. Of the expression changes in 22 genes in $Bcrp^{-/-}$ mice only a ~2-fold increase in solute carriers 3a1 and 41a2, which don't appear to play relevant roles in drug transport, and 3-fold decrease in the cytochrome P450 isoform 2b10 expression are of potential interest in the context of drug metabolism and disposition (Supplemental Table 3), but these changes do not preclude the general application of these mice. Further investigations will be needed to assess changes in other tissues.

Our studies confirmed the important role of Bcrp/BCRP in oral bioavailability and/or tissue distribution of sulfasalazine, daidzein, genistein, rosuvastatin and topotecan, as demonstrated by the various differences in pharmacokinetics and brain penetration of these compounds between WT, hBCRP and $Bcrp^{-/-}$ mice. Moreover, the functional activity of human BCRP in hBCRP mice was clearly shown by comparing the blood and tissue exposure of these BCRP probe substrates between the three mouse lines. In the case of sulfasalazine, the AUC after iv and po administration was increased significantly more in $Bcrp^{-/-}$ than in hBCRP mice when compared to WT controls (Supplemental Table 4A). In addition, the clearance and C_{max} of sulfasalazine were altered to a much lesser extent in hBCRP than in $Bcrp^{-/-}$ mice. Similar

Molecular Pharmacology Fast Forward. Published on February 18, 2016 as DOI: 10.1124/mol.115.102079
This article has not been copyedited and formatted. The final version may differ from this version.

observations were made for the plasma or blood concentrations of daidzein (Fig. 4A, B), genistein (Fig. 5A-C) and rosuvastatin (Fig. 6A, B, Supplemental Table 6), which were slightly increased in Bcrp$^{-/-}$ but not hBCRP mice relative to WT controls. Furthermore, the mean brain concentration and brain-to-plasma ratio of daidzein and genistein were significantly higher in Bcrp$^{-/-}$ compared to WT and hBCRP animals (Fig. 4C-E, Fig. 5D-F). Blood concentrations of topotecan in hBCRP mice after iv and po administration as well as brain concentrations 60 minutes after po dosing were also lower compared to Bcrp$^{-/-}$ animals, but the recovery towards WT levels was relatively weak (Fig. 7A, B, D, Supplemental Table 8). Based on our results the overall relevance of Bcrp/BCRP in restricting the brain penetration of the dual P-gp/BCRP substrate topotecan appears to be relatively low, which is in agreement with a previous study (de Vries et al., 2007) and can be attributed to the activity of P-gp compensating the loss of Bcrp. Accordingly, the higher $K_{b,\ brain}$ values at 15 and 60 minutes after po administration in WT compared to Bcrp$^{-/-}$ and hBCRP mice (Fig. 7E) are a consequence of the lower topotecan blood concentrations in WT mice, i.e. the relatively stronger effect of Bcrp in limiting oral bioavailability versus brain penetration. In summary, our data demonstrate that human BCRP is able to functionally compensate for the loss of mouse Bcrp in the hBCRP mice.

A consistent trend observed for all five probe substrates is that the blood concentrations in hBCRP mice never reach the levels observed in WT controls. This observation might be generally explained by the lower expression level of the transporter in the gut, liver and kidney of the humanized mice (Fig. 2), though species differences in the transport activity between murine Bcrp and human BCRP might contribute to this result for some of the compounds. The latter point might also explain why the pharmacokinetic profiles of sulfasalazine, rosuvastatin and topotecan in hBCRP mice vary in different ways from those observed in WT and Bcrp$^{-/-}$ mice. Furthermore, we cannot exclude that changes in the expression level of other transporters or drug metabolizing enzymes contribute to the

Molecular Pharmacology Fast Forward. Published on February 18, 2016 as DOI: 10.1124/mol.115.102079
This article has not been copyedited and formatted. The final version may differ from this version.

differences in the pharmacokinetic profiles in the hBCRP mice. However, based on the results from our microarray studies (Supplemental Table 3) such changes appear to be minimal and they are unlikely to be of major relevance. In contrast to the results observed for blood concentrations, daidzein and genistein brain concentrations were fully recovered (Fig. 4C-E, Fig. 5D-F), consistent with the similar expression level of Bcrp/BCRP in cortical vessels of WT and hBCRP mice (Fig. 2, Table 1). Interestingly, the topotecan brain concentration in hBCRP mice was 1.8-fold higher ($P<0.05$) than in WT mice 60 minutes after po administration (Fig. 7D). This observation might be attributed to a species difference in the topotecan transport activity of mouse Bcrp versus human BCRP, which could also explain the relatively weak recovery of blood concentrations in hBCRP mice (Fig 7A and B).

In addition to assessing substrate interactions with BCRP, studying DDIs caused by the inhibition of this transporter is a potentially valuable application of the hBCRP mice. In order to evaluate their utility for this type of application, we investigated the effect of the BCRP inhibitor Ko143 on oral bioavailability of sulfasalazine and brain penetration of tariquidar. Ko143 increased the blood concentrations, $AUC_{0\text{-}last}$ (and $AUC_{0\text{-}1}$) and C_{max} of sulfasalazine in WT and hBCRP but not $Bcrp^{-/-}$ animals (Fig. 3C, Supplemental Tables 4A and B), whereby the stronger inhibitory effect in WT compared to hBCRP mice might be attributed to the differences in the expression level of Bcrp/BCRP in the gut of these the two mouse lines. In agreement with the comparable expression level of Bcrp/BCRP at the BBB in WT and hBCRP mice, Ko143 increased the $K_{b,brain}$ value of tariquidar to a similar extent in both lines (Fig. 8E).

The present work describes the first generation and extensive characterization of a humanized BCRP mouse model. The results from these studies demonstrate the integrity and functionality of this novel model. The hBCRP mouse provides a valuable alternative or adjunct to WT animals in studies using Bcrp knockout mice or chemical inhibitors of

Molecular Pharmacology Fast Forward. Published on February 18, 2016 as DOI: 10.1124/mol.115.102079
This article has not been copyedited and formatted. The final version may differ from this version.

BCRP/Bcrp aiming to assess substrate or inhibitor in vivo interactions with BCRP, specifically where species differences are of concern. Though the results obtained with topotecan might indicate a difference in the topotecan transport activity of mouse Bcrp versus human BCRP (see above), the systematic analysis of species differences by using the hBCRP mice is beyond the scope of this work and will be subject to further investigations. Based on previously published work, fumitremorgin C could be considered as a potential inhibitor (Gonzalez-Lobato et al., 2010) and pheophorbide A or bisphenol A as substrates (2010; Li et al., 2008; Mazur et al., 2012) for such studies. Thus, the hBCRP mouse model provides a novel tool for identifying differences in inhibitor or substrate interactions with this transporter, either for basic research purposes or in drug development. With regards to the latter, this information, in conjunction with results obtained from in vitro studies and in Bcrp$^{-/-}$ mice, can help to estimate the potential need for clinical DDI studies.

Molecular Pharmacology Fast Forward. Published on February 18, 2016 as DOI: 10.1124/mol.115.102079
This article has not been copyedited and formatted. The final version may differ from this version.

Acknowledgements

We wish to thank Heidrun Kern and Steffen Guettler from Taconic Biosciences GmbH, Aysel Gueler, Ina Mairhofer and Klaus Magin from Abbvie, William Kintigh, Manna Manna, Christine Stewart, Stephen O'Sullivan (in vivo group) and Monica Singer from Janssen, Scott Fauty, Karen Owens, Gino Salituro from Merck Sharp & Dohme, the GlaxoSminthKline DMPK, Laboratory Animal Services and Statistics departments (Caroline Sychterz, JoAnn Coleman, Debra Paul, Edward Long, Deborah McCoy, Holly Sekellick and Leonard Azzarano), Meryam Taghi from Université Paris Descartes and the In Vivo Studies Group at Genentech for excellent technical assistance. We want to acknowledge Cerina Chhuon and Chiara Guerrera (Proteomic Platform Necker, Université Paris Descartes, Paris, France) for their services and help regarding the utilization of the UHPLC-MS/MS system for quantitative proteomics analysis. The authors would like to acknowledge the AIT imaging group (S. Mairinger, T. Filip, M. Sauberer, J. Stanek, A. Traxl and M. Löbsch) for support in performing the PET imaging part of this work.

Molecular Pharmacology Fast Forward. Published on February 18, 2016 as DOI: 10.1124/mol.115.102079
This article has not been copyedited and formatted. The final version may differ from this version.

Authorship Contributions

Participated in research design: DS, JK, JP, KD, LC, LL, LS, MM, NS, OL, SD, TW, XC, XD

Conducted experiments: AR, CA, CH, DGZ, EP, JP, JK, JY, MCM, MM, SC, TP, TW, XZ

Contributed new reagents or analytic tools: DGZ, MCM, XZ

Performed data analysis: CA, CH, DGZ, DS, EP, JK, JP, JY, KD, LC, LL, LS, MM, NS, MCM, OL, TP, TW, XC, XZ

Wrote or contributed to the writing of the manuscript: CA, DGZ, DS, EP, JK, KD, LC, KK, LS, MCM, MM, NS, OL, SD, TW, XC, XD

Molecular Pharmacology Fast Forward. Published on February 18, 2016 as DOI: 10.1124/mol.115.102079
This article has not been copyedited and formatted. The final version may differ from this version.

References

Allen JD, van Loevezijn A, Lakhai JM, van der Valk M, van Tellingen O, Reid G, Schellens JH, Koomen GJ and Schinkel AH (2002) Potent and specific inhibition of the breast cancer resistance protein multidrug transporter in vitro and in mouse intestine by a novel analogue of fumitremorgin C. *Mol Cancer Ther* **1**(6):417-425.

Bankstahl JP, Bankstahl M, Romermann K, Wanek T, Stanek J, Windhorst AD, Fedrowitz M, Erker T, Muller M, Loscher W, Langer O and Kuntner C (2013) Tariquidar and elacridar are dose-dependently transported by P-glycoprotein and Bcrp at the blood-brain barrier: a small-animal positron emission tomography and in vitro study. *Drug Metab Dispos* **41**(4):754-762.

Behringer R, Gertsenstein M, Nagy KV and Nagy A (2014) Manipulating the Mouse Embryo - A Laboratory Manual. *Cold Spring Harbor Laboratory Press* **Fourth Edition**:321-485.

Chambers KJ, Tonkin LA, Chang E, Shelton DN, Linskens MH and Funk WD (1998) Identification and cloning of a sequence homologue of dopamine beta-hydroxylase. *Gene* **218**(1-2):111-120.

Chan LM, Lowes S and Hirst BH (2004) The ABCs of drug transport in intestine and liver: efflux proteins limiting drug absorption and bioavailability. *Eur J Pharm Sci* **21**(1):25-51.

Chu X, Bleasby K and Evers R (2013) Species differences in drug transporters and implications for translating preclinical findings to humans. *Expert Opin Drug Metab Toxicol* **9**(3):237-252.

de Vries NA, Zhao J, Kroon E, Buckle T, Beijnen JH and van Tellingen O (2007) P-glycoprotein and breast cancer resistance protein: two dominant transporters working together in limiting the brain penetration of topotecan. *Clin Cancer Res* **13**(21):6440-6449.

Doyle L and Ross DD (2003) Multidrug resistance mediated by the breast cancer resistance protein BCRP (ABCG2). *Oncogene* **22**(47):7340-7358.

Enokizono J, Kusuhara H and Sugiyama Y (2007) Effect of Breast Cancer Resistance Protein (Bcrp/Abcg2) on the Disposition of Phytoestrogens. *Molecular Pharmacology* **72**(4):967-975.

European Medicine Agency (EMA) CfHMPC (2012) Guideline on the investigation of drug interactions. 21 June 2012.

Giacomini KM, Huang SM, Tweedie DJ, Benet LZ, Brouwer KL, Chu X, Dahlin A, Evers R, Fischer V, Hillgren KM, Hoffmaster KA, Ishikawa T, Keppler D, Kim RB, Lee CA, Niemi M, Polli JW, Sugiyama Y, Swaan PW, Ware JA, Wright SH, Yee SW, Zamek-Gliszczynski MJ and Zhang L (2010) Membrane transporters in drug development. *Nat Rev Drug Discov* **9**(3):215-236.

Gonzalez-Lobato L, Real R, Prieto JG, Alvarez AI and Merino G (2010) Differential inhibition of murine Bcrp1/Abcg2 and human BCRP/ABCG2 by the mycotoxin fumitremorgin C. *Eur J Pharmacol* **644**(1-3):41-48.

Hoshi Y, Uchida Y, Tachikawa M, Inoue T, Ohtsuki S and Terasaki T (2013) Quantitative atlas of blood-brain barrier transporters, receptors, and tight junction proteins in rats and common marmoset. *J Pharm Sci* **102**(9):3343-3355.

Hua WJ, Hua WX and Fang HJ (2012) The role of OATP1B1 and BCRP in pharmacokinetics and DDI of novel statins. *Cardiovasc Ther* **30**(5):e234-241.

Jani M, Makai I, Kis E, Szabo P, Nagy T, Krajcsi P and Lespine A (2011) Ivermectin interacts with human ABCG2. *J Pharm Sci* **100**(1):94-97.

Jonker JW, Buitelaar M, Wagenaar E, Van Der Valk MA, Scheffer GL, Scheper RJ, Plosch T,

Kuipers F, Elferink RP, Rosing H, Beijnen JH and Schinkel AH (2002) The breast cancer resistance protein protects against a major chlorophyll-derived dietary phototoxin and protoporphyria. *Proc Natl Acad Sci U S A* **99**(24):15649-15654.

Jonker JW, Smit JW, Brinkhuis RF, Maliepaard M, Beijnen JH, Schellens JH and Schinkel AH (2000) Role of breast cancer resistance protein in the bioavailability and fetal penetration of topotecan. *J Natl Cancer Inst* **92**(20):1651-1656.

Kamiie J, Ohtsuki S, Iwase R, Ohmine K, Katsukura Y, Yanai K, Sekine Y, Uchida Y, Ito S and Terasaki T (2008) Quantitative atlas of membrane transporter proteins: development and application of a highly sensitive simultaneous LC/MS/MS method combined with novel in-silico peptide selection criteria. *Pharm Res* **25**(6):1469-1483.

Kannan P, Telu S, Shukla S, Ambudkar SV, Pike VW, Halldin C, Gottesman MM, Innis RB and Hall MD (2011) The "specific" P-glycoprotein inhibitor Tariquidar is also a substrate and an inhibitor for breast cancer resistance protein (BCRP/ABCG2). *ACS Chem Neurosci* **2**(2):82-89.

Kitamura S, Maeda K, Wang Y and Sugiyama Y (2008) Involvement of multiple transporters in the hepatobiliary transport of rosuvastatin. *Drug Metab Dispos* **36**(10):2014-2023.

Kodaira H, Kusuhara H, Ushiki J, Fuse E and Sugiyama Y (2010) Kinetic analysis of the cooperation of P-glycoprotein (P-gp/Abcb1) and breast cancer resistance protein (Bcrp/Abcg2) in limiting the brain and testis penetration of erlotinib, flavopiridol, and mitoxantrone. *J Pharmacol Exp Ther* **333**(3):788-796.

Kusuhara H, Furuie H, Inano A, Sunagawa A, Yamada S, Wu C, Fukizawa S, Morimoto N, Ieiri I, Morishita M, Sumita K, Mayahara H, Fujita T, Maeda K and Sugiyama Y (2012) Pharmacokinetic interaction study of sulphasalazine in healthy subjects and the impact of curcumin as an in vivo inhibitor of BCRP. *Br J Pharmacol* **166**(6):1793-1803.

Lagas JS, van Waterschoot RA, Sparidans RW, Wagenaar E, Beijnen JH and Schinkel AH (2010) Breast cancer resistance protein and P-glycoprotein limit sorafenib brain accumulation. *Mol Cancer Ther* **9**(2):319-326.

Lai Y (2009) Identification of interspecies difference in hepatobiliary transporters to improve extrapolation of human biliary secretion. *Expert Opin Drug Metab Toxicol* **5**(10):1175-1187.

Lee SS, Jeong HE, Yi JM, Jung HJ, Jang JE, Kim EY, Lee SJ and Shin JG (2007) Identification and functional assessment of BCRP polymorphisms in a Korean population. *Drug Metab Dispos* **35**(4):623-632.

Leggas M, Adachi M, Scheffer GL, Sun D, Wielinga P, Du G, Mercer KE, Zhuang Y, Panetta JC, Johnston B, Scheper RJ, Stewart CF and Schuetz JD (2004) Mrp4 confers resistance to topotecan and protects the brain from chemotherapy. *Mol Cell Biol* **24**(17):7612-7621.

Leslie EM, Deeley RG and Cole SP (2005) Multidrug resistance proteins: role of P-glycoprotein, MRP1, MRP2, and BCRP (ABCG2) in tissue defense. *Toxicol Appl Pharmacol* **204**(3):216-237.

Li M, Yuan H, Li N, Song G, Zheng Y, Baratta M, Hua F, Thurston A, Wang J and Lai Y (2008) Identification of interspecies difference in efflux transporters of hepatocytes from dog, rat, monkey and human. *Eur J Pharm Sci* **35**(1-2):114-126.

Li N, Palandra J, Nemirovskiy OV and Lai Y (2009) LC-MS/MS mediated absolute quantification and comparison of bile salt export pump and breast cancer resistance protein in livers and hepatocytes across species. *Anal Chem* **81**(6):2251-2259.

Mazur CS, Marchitti SA, Dimova M, Kenneke JF, Lumen A and Fisher J (2012) Human and rat ABC transporter efflux of bisphenol a and bisphenol a glucuronide: interspecies comparison and implications for pharmacokinetic assessment. *Toxicol Sci* **128**(2):317-325.

Molecular Pharmacology Fast Forward. Published on February 18, 2016 as DOI: 10.1124/mol.115.102079
This article has not been copyedited and formatted. The final version may differ from this version.

Meyer zu Schwabedissen HE and Kroemer HK (2011) In vitro and in vivo evidence for the importance of breast cancer resistance protein transporters (BCRP/MXR/ABCP/ABCG2). *Handb Exp Pharmacol*(201):325-371.

Ni Z, Bikadi Z, Rosenberg MF and Mao Q (2010) Structure and function of the human breast cancer resistance protein (BCRP/ABCG2). *Curr Drug Metab* **11**(7):603-617.

Rostami-Hodjegan A (2012) Physiologically based pharmacokinetics joined with in vitro-in vivo extrapolation of ADME: a marriage under the arch of systems pharmacology. *Clin Pharmacol Ther* **92**(1):50-61.

Sadiq MW, Uchida Y, Hoshi Y, Tachikawa M, Terasaki T and Hammarlund-Udenaes M (2015) Validation of a P-Glycoprotein (P-gp) Humanized Mouse Model by Integrating Selective Absolute Quantification of Human MDR1, Mouse Mdr1a and Mdr1b Protein Expressions with In Vivo Functional Analysis for Blood-Brain Barrier Transport. *PLoS One* **10**(5):e0118638.

Silamut K, Molunto P, Ho M, Davis TM and White NJ (1991) Alpha 1-acid glycoprotein (orosomucoid) and plasma protein binding of quinine in falciparum malaria. *Br J Clin Pharmacol* **32**(3):311-315.

U.S. Department of Health and Human Services FaDA, Center for Drug Evaluation and Research (CDER). (2012.) Guidance for industry, drug interaction studies—study design, data analysis, implications for dosing, and labeling recommendations. . *http://wwwfdagov/downloads/Drugs/GuidanceComplianceRegulatoryInformation/Guidances/ucm292362pdf*.

Uchida Y, Ohtsuki S, Katsukura Y, Ikeda C, Suzuki T, Kamiie J and Terasaki T (2011) Quantitative targeted absolute proteomics of human blood-brain barrier transporters and receptors. *J Neurochem* **117**(2):333-345.

Urquhart BL, Ware JA, Tirona RG, Ho RH, Leake BF, Schwarz UI, Zaher H, Palandra J, Gregor JC, Dresser GK and Kim RB (2008) Breast cancer resistance protein (ABCG2) and drug disposition: intestinal expression, polymorphisms and sulfasalazine as an in vivo probe. *Pharmacogenet Genomics* **18**(5):439-448.

Wanek T, Kuntner C, Bankstahl JP, Mairinger S, Bankstahl M, Stanek J, Sauberer M, Filip T, Erker T, Muller M, Loscher W and Langer O (2012) A novel PET protocol for visualization of breast cancer resistance protein function at the blood-brain barrier. *J Cereb Blood Flow Metab* **32**(11):2002-2011.

Warren MS, Zerangue N, Woodford K, Roberts LM, Tate EH, Feng B, Li C, Feuerstein TJ, Gibbs J, Smith B, de Morais SM, Dower WJ and Koller KJ (2009) Comparative gene expression profiles of ABC transporters in brain microvessel endothelial cells and brain in five species including human. *Pharmacol Res* **59**(6):404-413.

Yamasaki Y, Ieiri I, Kusuhara H, Sasaki T, Kimura M, Tabuchi H, Ando Y, Irie S, Ware J, Nakai Y, Higuchi S and Sugiyama Y (2008) Pharmacogenetic characterization of sulfasalazine disposition based on NAT2 and ABCG2 (BCRP) gene polymorphisms in humans. *Clin Pharmacol Ther* **84**(1):95-103.

Zaher H, Khan AA, Palandra J, Brayman TG, Yu L and Ware JA (2006) Breast cancer resistance protein (Bcrp/abcg2) is a major determinant of sulfasalazine absorption and elimination in the mouse. *Mol Pharm* **3**(1):55-61.

Zamek-Gliszczynski MJ, Bedwell DW, Bao JQ and Higgins JW (2012a) Characterization of SAGE Mdr1a (P-gp), Bcrp, and Mrp2 knockout rats using loperamide, paclitaxel, sulfasalazine, and carboxydichlorofluorescein pharmacokinetics. *Drug Metab Dispos* **40**(9):1825-1833.

Zamek-Gliszczynski MJ, Hoffmaster KA, Tweedie DJ, Giacomini KM and Hillgren KM (2012b) Highlights from the International Transporter Consortium second workshop. *Clin Pharmacol Ther* **92**(5):553-556.

Zhang W, Yu BN, He YJ, Fan L, Li Q, Liu ZQ, Wang A, Liu YL, Tan ZR, Fen J, Huang YF

Molecular Pharmacology Fast Forward. Published on February 18, 2016 as DOI: 10.1124/mol.115.102079
This article has not been copyedited and formatted. The final version may differ from this version.

and Zhou HH (2006) Role of BCRP 421C>A polymorphism on rosuvastatin pharmacokinetics in healthy Chinese males. *Clin Chim Acta* **373**(1-2):99-103.

Zhang Y, Buchholz F, Muyrers JP and Stewart AF (1998) A new logic for DNA engineering using recombination in Escherichia coli. *Nat Genet* **20**(2):123-128.

Molecular Pharmacology Fast Forward. Published on February 18, 2016 as DOI: 10.1124/mol.115.102079
This article has not been copyedited and formatted. The final version may differ from this version.

Footnotes

SD and LS contributed equally to this paper.

The PET imaging part of this work was supported by the Austrian Science fund (FWF) [Grants P24894-B24 and F 3513-B20].

Reprint requests:

Laurent Salphati, Pharm.D., PhD, Department of Drug Metabolism and Pharmacokinetics, Genentech, Inc., 1 DNA Way, South San Francisco, CA 94080, USA.

Tel.: 650-467-1796; Fax: 650-467-3487; Email: salphati.laurent@gene.com

Molecular Pharmacology Fast Forward. Published on February 18, 2016 as DOI: 10.1124/mol.115.102079
This article has not been copyedited and formatted. The final version may differ from this version.

Figure Legends

Fig. 1 Strategy to generate hBCRP and Bcrp$^{-/-}$ mice. (A) Genomic organisation of the mouse *Bcrp* gene locus. The start ATG and stop codon are shown. (B) Vector used for targeting of *Bcrp* by homologous recombination in mouse ES cells. (C) Genomic organisation of *Bcrp* in targeted ES cells after homologous recombination. (D) *Bcrp* gene locus in the hBCRP model after Flp-mediated deletion of the neomycin (Neo) and puromycin (Puro) expression cassettes. (E) *Bcrp* gene locus in the Bcrp$^{-/-}$ model after Cre-mediated deletion of human *BCRP* exons 3-15. For the sake of clarity sequences of the targeting vectors are not drawn to scale.

Fig. 2 Relative murine *Bcrp* and human *BCRP* mRNA expression levels in WT and hBCRP mice. RNA was isolated from WT and hBCRP male (black bars) and female (grey bars) mice (n=3 for each line and sex). Murine *Bcrp* and human *BCRP* mRNA expression was analyzed by quantitative PCR (TaqMan) in liver (A), brain (B), kidney (C), duodenum (D), colon (E) and testis (F) and normalized to murine β-actin. Relative mRNA levels were assessed by a comparative ($2^{-\Delta\Delta CT}$) approach as described in the Supplemental Materials and Methods section. Values represent the mean expression level ± SD with expression levels of the murine *Bcrp* mRNA in WT males arbitrarily set as 1.

Fig. 3 Sulfasalazine blood concentration-time profiles in WT, hBCRP and Bcrp$^{-/-}$ mice. Pharmacokinetic profile after 5 mg/kg iv (A) or 20 mg po (B, C) administration of sulfasalazine to male WT (black diamond), hBCRP mice (dark grey triangle) and Bcrp1$^{-/-}$ (light grey circle). Sulfasalazine was administered in the absence (A, B) or presence (C) of the BCRP inhibitor Ko143 (20 mg/kg). Sulafasalazine concentrations-time profiles in the presence of Ko143 are represented as dotted lines (C). Values shown are mean ± SD of n=4

Molecular Pharmacology Fast Forward. Published on February 18, 2016 as DOI: 10.1124/mol.115.102079
This article has not been copyedited and formatted. The final version may differ from this version.

mice per strain.

Fig. 4 Daidzein plasma concentration-time profiles and brain and plasma concentrations in WT, hBCRP and Bcrp$^{-/-}$ mice. 5 mg/kg daidzein was administered IV to male mice. (A) Pharmacokinetic profiles in WT (black triangles), hBCRP (dark grey diamonds) and Bcrp$^{-/-}$ mice (light grey squares). (B) $AUC_{0\text{-}1hr}$ values in WT (black bar), hBCRP (dark grey bar) and Bcrp$^{-/-}$ mice (light grey bar). (C-E) Plasma (black bars) and brain (grey bars) concentrations at (C) 30 minutes, (D) 1 hour and (E) 2 hours after daidzein administration. Values shown in (A) and (C-E) are mean ± SD with n=3 mice per strain and time point for (A) and n=2 mice per strain and time point for (C-E). *, $P < 0.05$, statistically significant compared to indicated control mice. $AUC_{0\text{-}1hr}$ (B) are mean (±SD; n=3 mice per strain); *, $P<0.05$, statistically significant compared to indicated control mice.

Fig. 5 Genistein blood concentration-time profiles and brain and blood concentrations in WT, hBCRP and Bcrp$^{-/-}$ mice. Pharmacokinetic profiles in WT (black circles), hBCRP (black triangles) and Bcrp$^{-/-}$ male mice (white circles) following (A) 20 mg/kg intravenous, (B) 20 mg/kg oral or (C) 50 mg/kg oral administration of genistein, respectively. (D and E) Genistein blood (black bars) and brain (grey bars) concentrations (D) 15 minutes and (E) 90 minutes after 20 mg/kg intravenous administration. (F) Genistein brain-to-blood concentration ratio in WT (black bars), hBCRP (grey bars) and Bcrp$^{-/-}$ (white bars) mice 15 and 90 minutes after 20 mg/kg intravenous administration. Values shown are mean ± SD with n=8 (A-C) or n=4 (D-F) mice per strain and time point. *, $P < 0.05$, statistically significant compared to Bcrp$^{-/-}$ mice.

Fig. 6 Rosuvastatin blood concentration-time profiles in WT, hBCRP and Bcrp$^{-/-}$ mice. Pharmacokinetic profiles in WT (black diamonds), hBCRP (black triangles) and Bcrp$^{-/-}$ male mice (white squares) following (A) 6.1 mg/kg intravenous and (B) 13.7 mg/kg oral

Molecular Pharmacology Fast Forward. Published on February 18, 2016 as DOI: 10.1124/mol.115.102079
This article has not been copyedited and formatted. The final version may differ from this version.

administration of rosuvastatin, respectively. Values shown are mean ± SD with n=4 mice per strain and time point.

Fig. 7 Topotecan blood concentration-time profiles and brain and blood concentrations in WT, hBCRP and Bcrp$^{-/-}$ mice. Pharmacokinetic profiles in WT (black diamonds), hBCRP (black triangles) and Bcrp$^{-/-}$ male mice (white squares) following (A) 1 mg/kg intravenous or (B) 1 mg/kg oral administration of topotecan, respectively. (C and D) Topotecan brain concentrations (C) 15 and (D) 60 minutes after 1 mg/kg oral administration. (E) Topotecan brain-to-blood concentration ratio in WT (black bars), hBCRP (grey bars) and Bcrp$^{-/-}$ (white bars) mice 15 and 60 minutes after 1 mg/kg oral administration. Values shown are mean ± SD with n=8 for WT and hBCRP and n=7 for Bcrp$^{-/-}$ (A), n=8 for Bcrp$^{-/-}$ and hBCRP and n=7 for WT (B), n=4 for each mouse line (C), n=4 for Bcrp$^{-/-}$ and hBCRP and n=3 for WT (D), and n=4 for WT and Bcrp$^{-/-}$ at 15 minutes and Bcrp$^{-/-}$ at 60 minutes and n=3 for WT at 60 minutes and hBCRP at 15 and 60 minutes. *, $P < 0.05$, statistically significant compared to Bcrp$^{-/-}$ mice.

Fig. 8 Sagittal PET summation images (0-60 min) and mean (± SD) time-activity curves of [^{11}C]tariquidar in hBCRP (A, B) and C57BL/6N WT mice (C, D) pretreated iv with tariquidar (TQD) and Ko143 vehicle (veh/veh) or tariquidar (12 mg/kg) and Ko143 vehicle (TQD/veh) or tariquidar (12 mg/kg) and Ko143 (10 mg/kg) (TQD/Ko143) (n = 4-6 per group). Tariquidar was administered at 2 hours and Ko143 at 1 hour before start of the PET scan. Whole brain region which was used for image quantification is highlighted (red broken line). All images are set to the same intensity scale (0-4 standardized uptake value, SUV). In (E) mean (+SD) brain-to-blood radioactivity concentration ratios at the end of the PET scan ($K_{b,brain}$) are shown (***, $P<0.001$, 1-way ANOVA followed by Bonferroni´s multiple comparison test).

Molecular Pharmacology Fast Forward. Published on February 18, 2016 as DOI: 10.1124/mol.115.102079
This article has not been copyedited and formatted. The final version may differ from this version.

Tables

TABLE 1

Expression of BCRP/Bcrp and Na^+/K^+ ATPase proteins in mouse Kidney, Liver and Cortical vessels obtained by AQUA quantification by UHPLC-MS/MS.

		Expression per sample group in fmol/µg of total protein (%CV)	
Tissue	**Mouse line**	**Bcrp/BCRP**	**Na+/K+ ATPase**
Liver (PMF)	WT	1.55 (7.6%)	15.6 (8.9%)
	hBCRP	0.726 (12.6%)	17.1 (8.63%)
Kidney (PMF)	WT	37.7 (9.07%)	317 (24.9%)
	hBCRP	9.34 (14.5%)	231 (13.6%)
Cortical vessels (WL)	WT	0.225 (44.0%)	26.4 (31.9%)
	hBCRP	0.393 (17.4%)	29.1 (32.9%)

PMF = plasma membrane fraction; WL = whole lysate

Data are presented as the mean of the calculated value for the digestion replicates of each sample. Therefore, the %CV represents the variability between samples and digestion replicates. The analytical %CV corresponding to the digestion reproducibility was inferior to 20% in all the samples. For liver and kidney samples from 3 different mice per line were used and each sample was digested in triplicate. For cortical vessels samples from 2 WT and 3 hBCRP mice were used and each sample was digested from one to three replicates, depending on the protein amount obtained after vessel isolation.

Figure 1

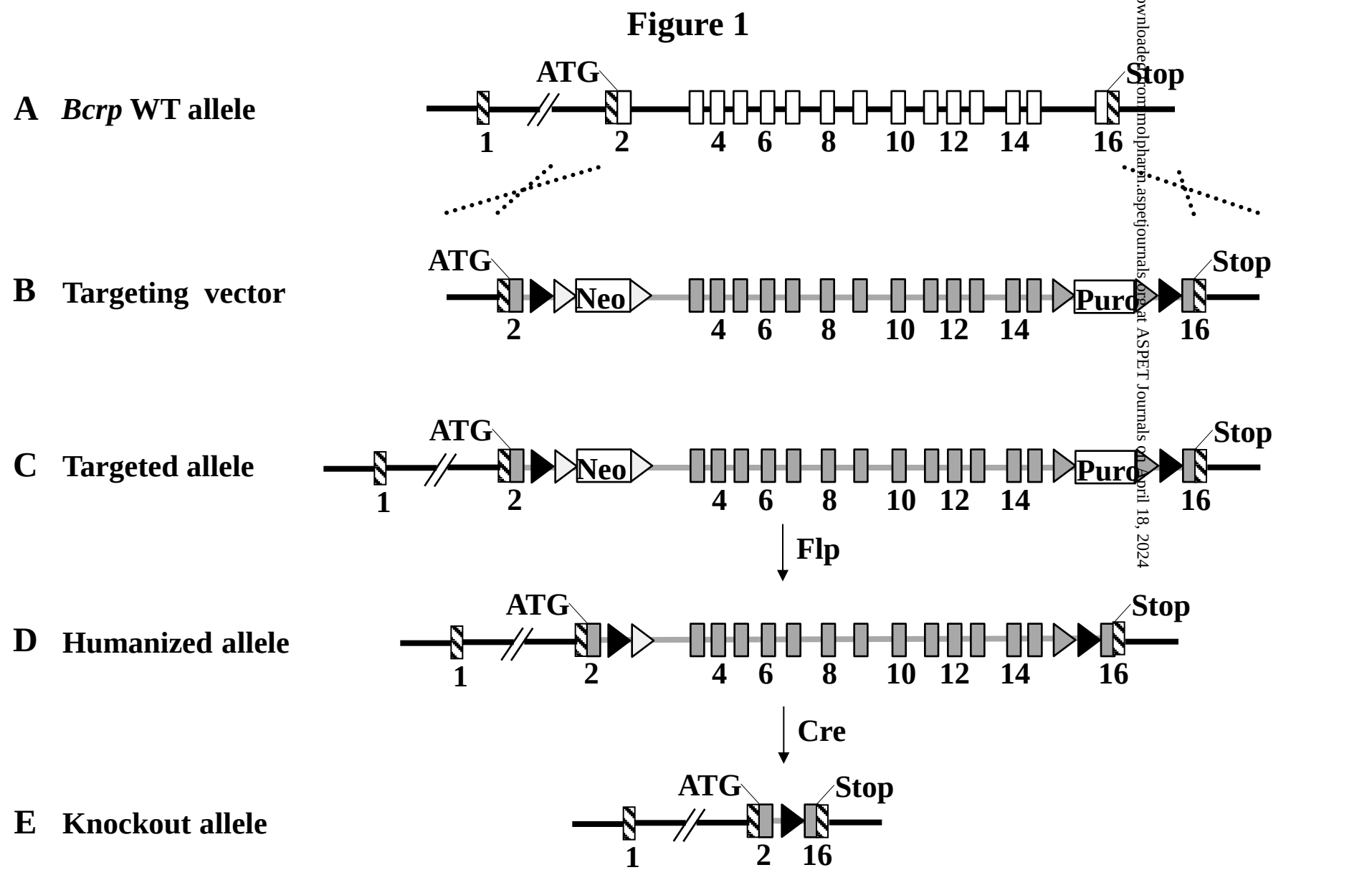

Figure 2

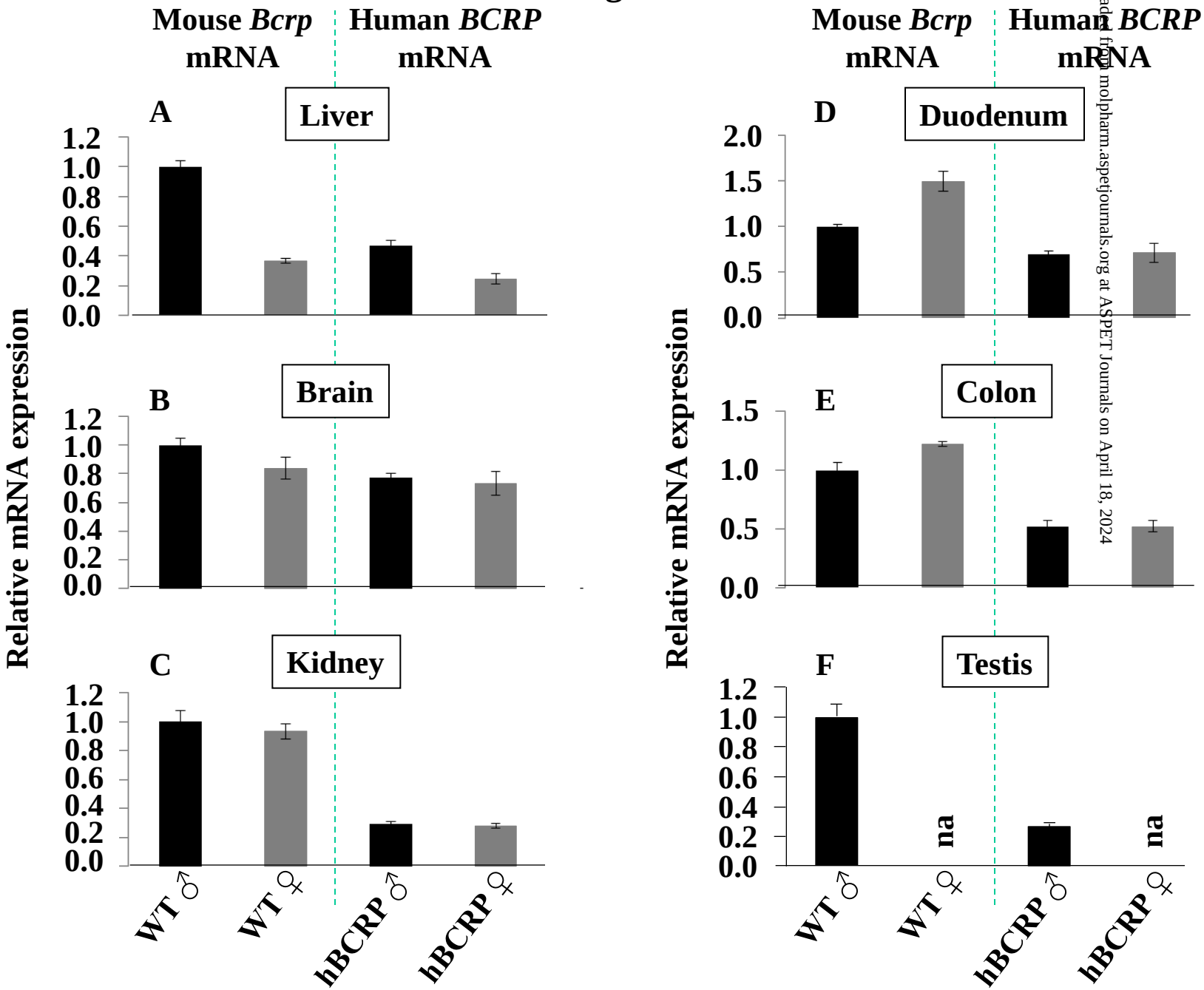

Figure 3

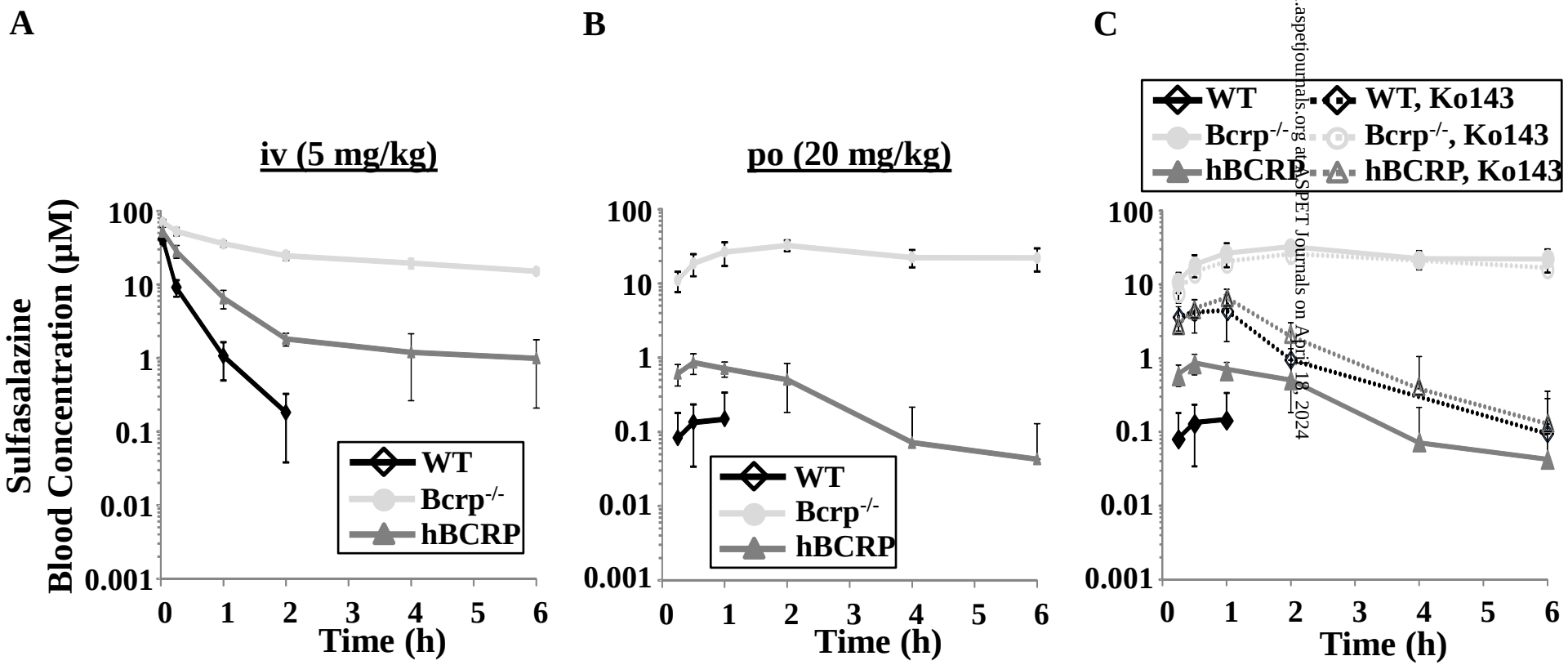

Figure 4

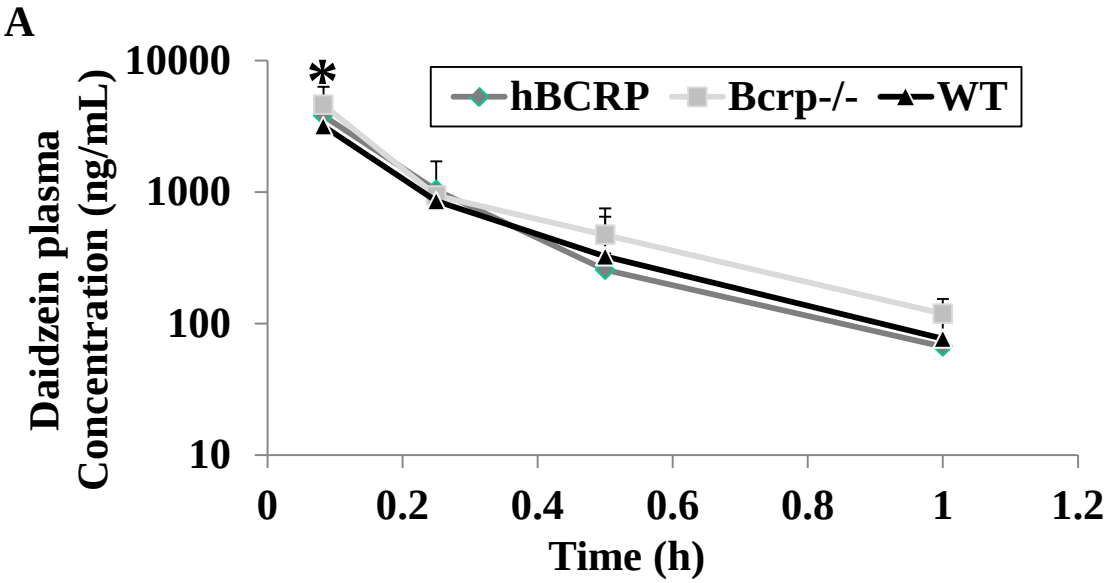

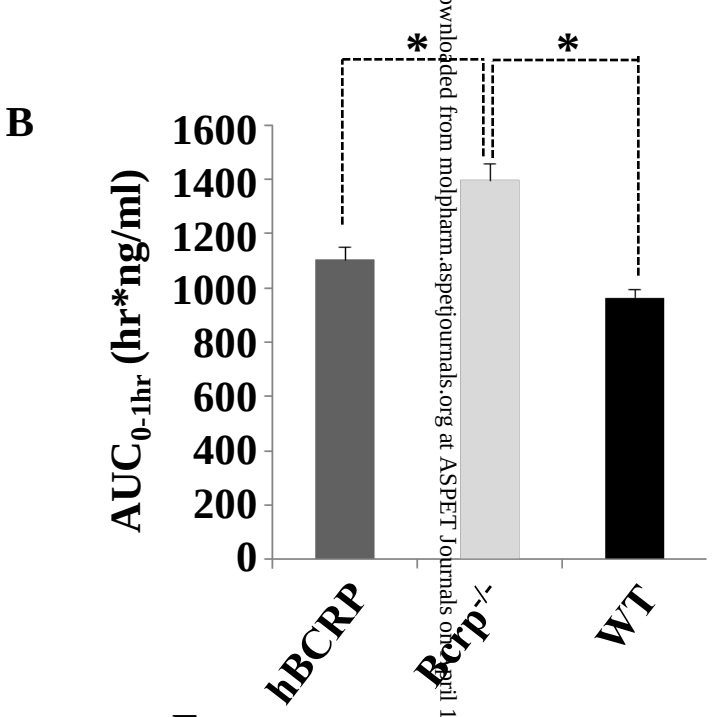

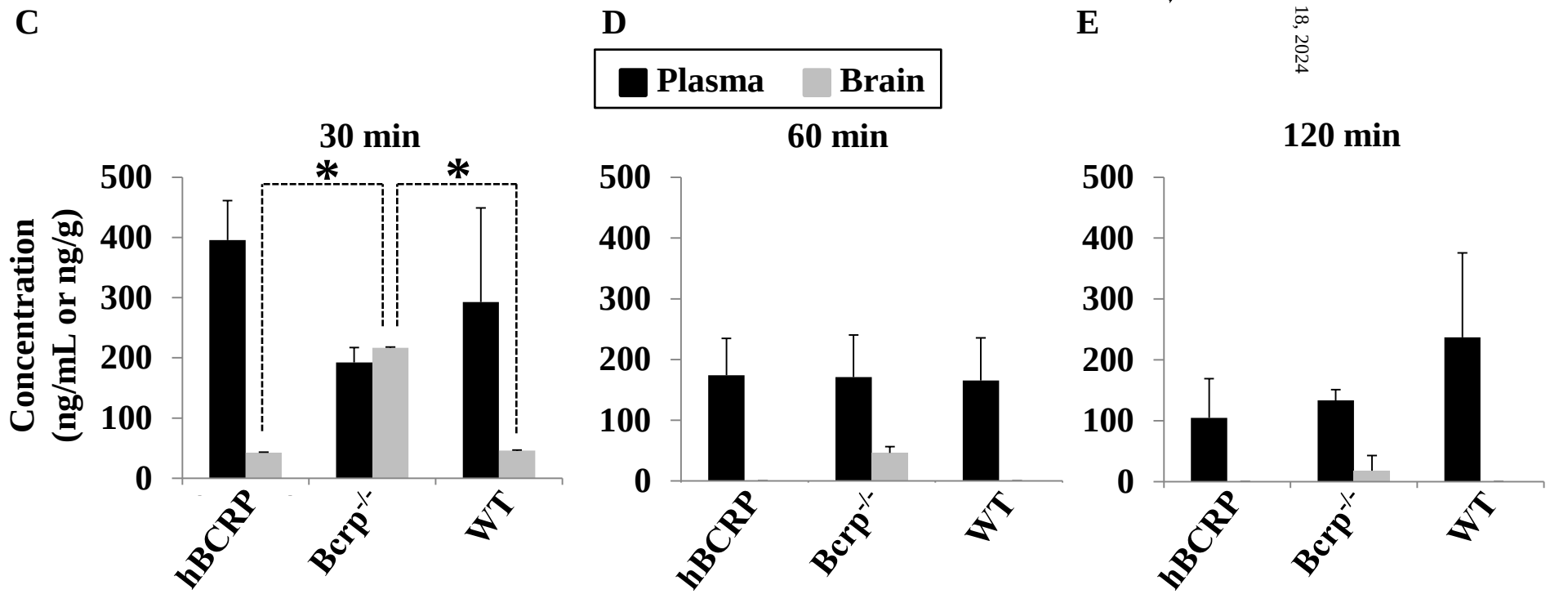

Figure 5

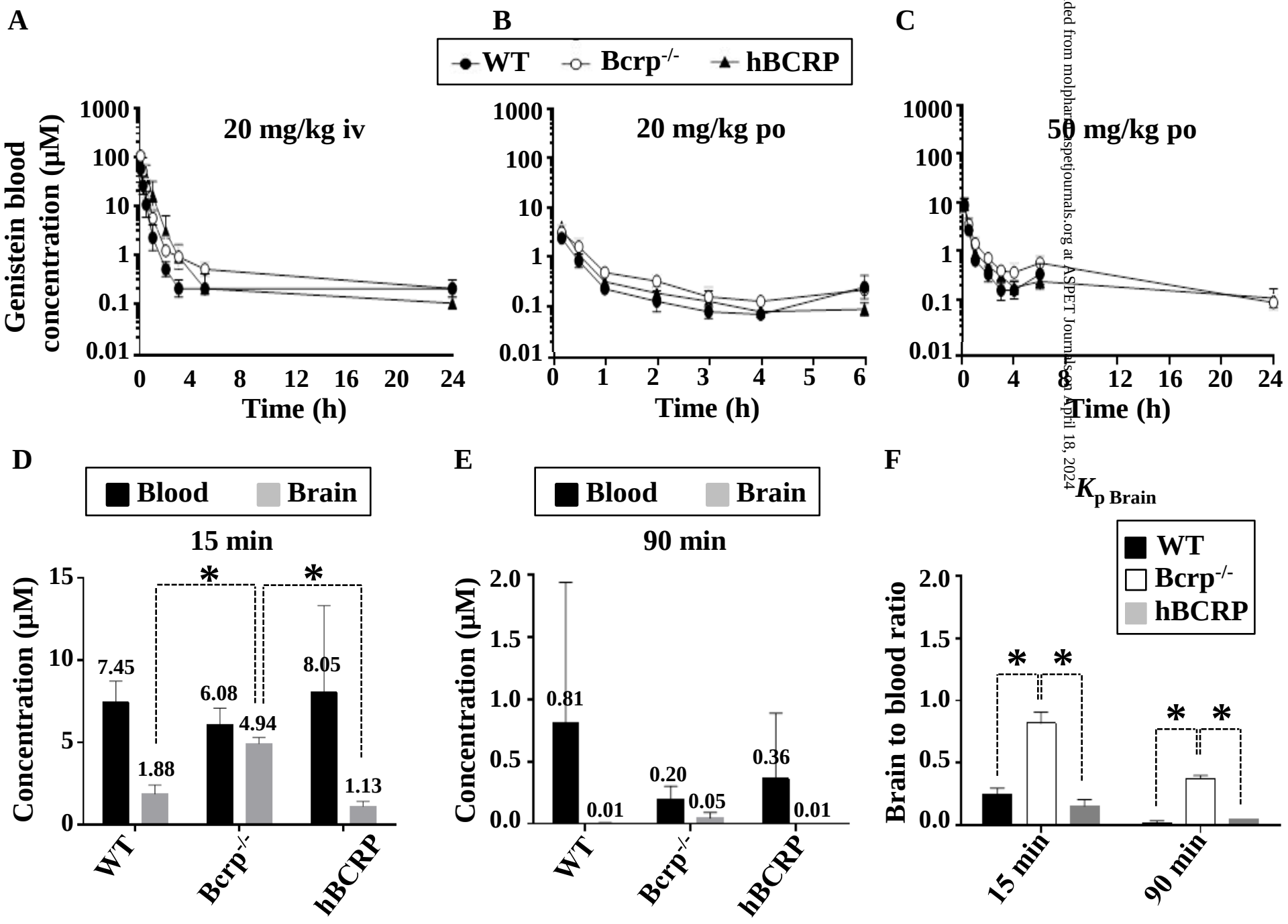

Figure 6

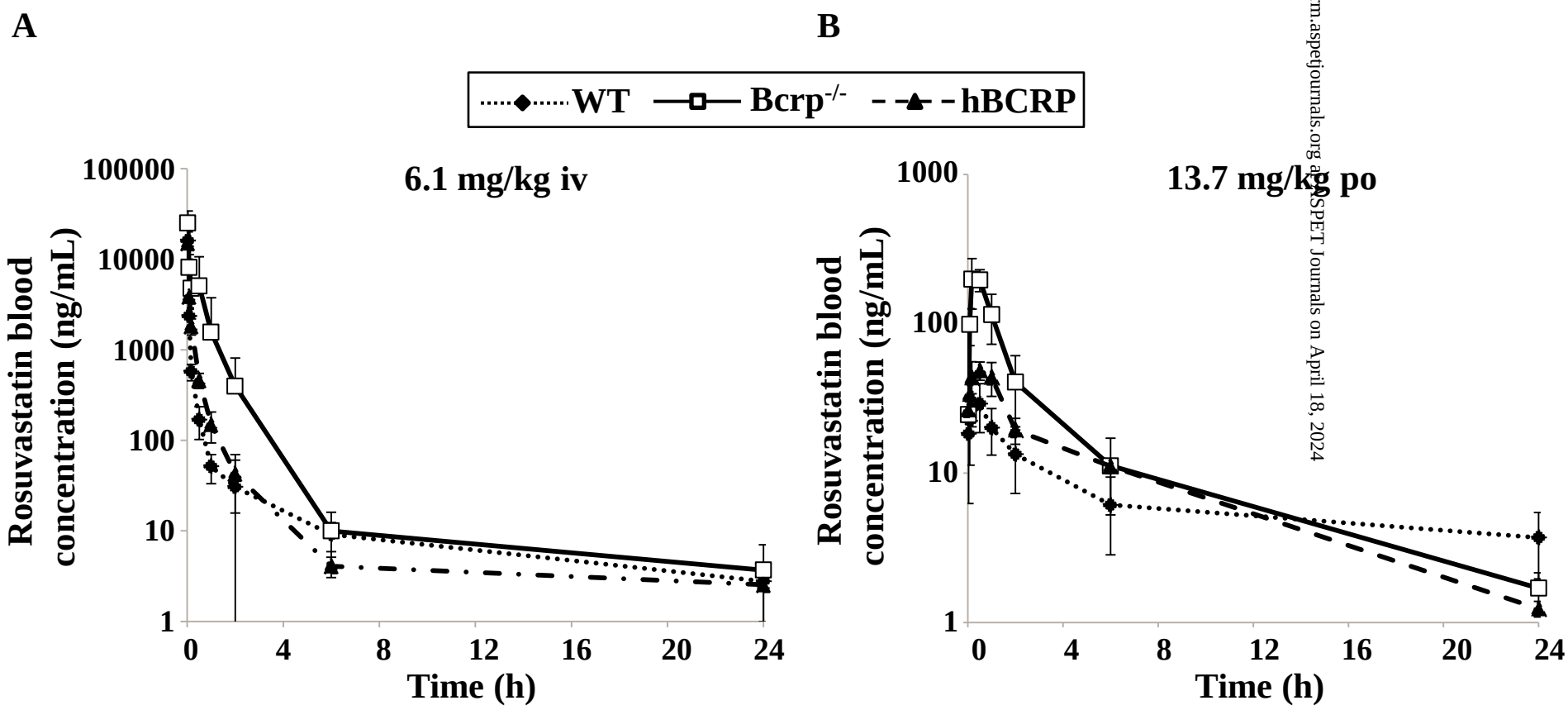

Figure 7

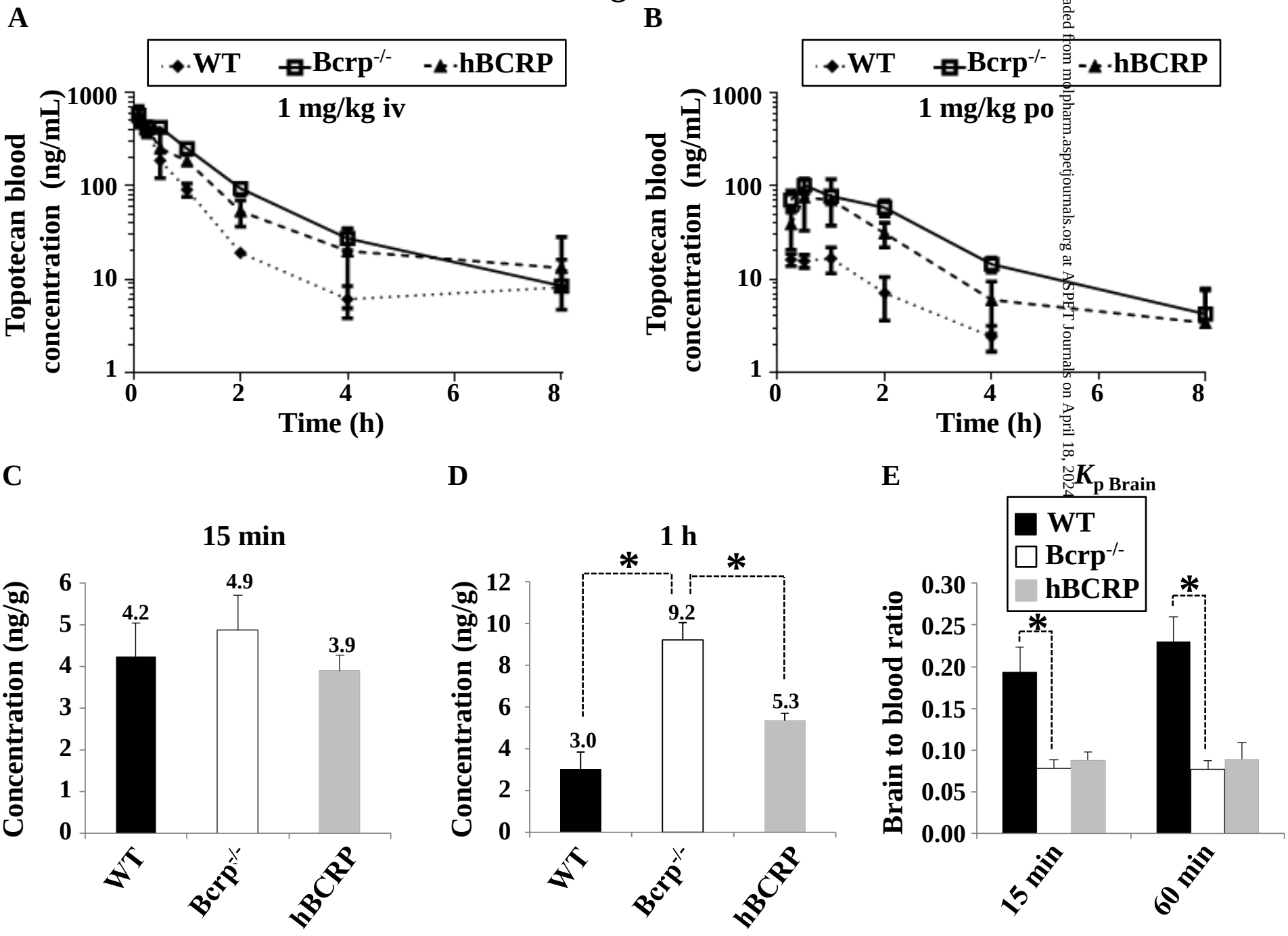

Supplemental Materials and Data

Generation and Characterization of a Breast Cancer Resistance Protein Humanized Mouse Model

Shannon Dallas, Laurent Salphati, David Gomez-Zepeda, Thomas Wanek, Liangfu Chen, Xiaoyan Chu, Jeevan Kunta, Mario Mezler, Marie-Claude Menet, Stephanie Chasseigneaux, Xavier Declèves, Oliver Langer, Esaie Pierre, Karen DiLoreto, Carolin Hoft, Loic Laplanche, Jodie Pang, Tony Pereira, Clara Andonian, Damir Simic, Anja Rode, Jocelyn Yabut, Xiaolin Zhang and Nico Scheer

Molecular Pharmacology

Supplemental Materials and Methods

Quantitative Reverse Transcriptase PCR (qRT-PCR). mRNA expression was analyzed by quantitative RT-PCR (TaqMan). Total RNA was prepared as described previously (Scheer et al., 2012). cDNA was synthesized from 1µg total RNA using the Quantiscript Reverse Transcriptase Kit (QIAGEN). Primers used were from the following Assay-On-Demand Kits; mouse *Bcrp* Mm00496364_m1, human *BCRP* Hs01053790_m1, and mouse β-actin Mm00607939_m1 (Applied Biosystems, Foster City, CA). Quantitative RT-PCR reactions were performed using TaqMan Universal PCR Mastermix in an ABI PRISM 7000 Sequence Detection System (Applied Biosystems, Foster City, CA). Data were analyzed using comparative cycling time methodology, in which fluorescent output, measured as Ct, was directly proportional to input cDNA concentration. A Ct value of >38 was interpreted as absence of gene expression. Input cDNA concentrations were normalized to murine β-actin. Calculations were performed by a comparative method ($2^{-\Delta\Delta CT}$).

Affymetrix expression profiling (Microarray Analysis). Total RNA was prepared from flash frozen liver samples using RNeasy midi RNA preparation kit from Qiagen (Hilden, Germany) according to the manufacturer's instruction. Briefly, samples were homogenized in buffer RLT containing 1% b-mercaptoethanol (Sigma, St. Louis, MO). An equal volume of 70% ethanol was added and samples were added to the column. Columns were washed according to protocol and an on-column DNAse I digestion was included to reduce genomic DNA contamination. RNA was eluted with 500 µL RNAse free water. Quality was determined by Agilent's Bioanalyzer 2100 nano chip (Agilent Technologies, Santa Clara, CA) and quantity was determined via a NanoDrop 2000 (Thermo Scientific, Waltham, MA). All RNA samples displaying no visible degradation in the Bioanalyzer analysis with two sharp ribosomal peaks (18S and 28S) were deemed acceptable for further processing. Affymetrix's

GeneChip IVT Express kit was used for cDNA synthesis and *in vitro* transcription. An Affymetrix GeneChip Mouse Genome 430 2.0 Array was used in this study with data processed by the Affymetrix software Command Console and Expression Console using MAS5.0 Analysis Algorithms.

Cortical vessel isolation, preparation of plasma membrane fraction from different tissues, protein digestion and quantification by UHPLC-MS/MS. *Cortical vessel isolation and preparation of plasma membrane fraction:* Brain cortical vessels were isolated as described previously, with modifications (Dauchy et al., 2008; Yousif et al., 2007). Brains stored at -80°C, were thawed at +4°C. The cortices were dissected and the grey and white matters and the meninges were removed. For each sample, 5 brain cortexes were pooled and minced in 30 mL of buffer 1 (HBSS and 10 mM HEPES). The suspension obtained was centrifuged (600 g, 5 min, +4°C) and the resulting pellet suspended in buffer 1 supplemented with an enzymatic mixture. After incubation (37°C) and centrifugation (5,000 g, +4°C), the vessel-enriched pellet was suspended in buffer 2 (buffer 1 with 17.5% (w/w) dextran) and centrifuged for 30 min at 4500 g in a swinging bucket rotor. The resulting pellet was resuspended in buffer 3 (buffer 1 containing 1% (w/v) BSA) and passed through a 10-µm nylon mesh. The vessels retained on the nylon mesh were recovered in buffer 3 and centrifuged again (600 g, 5 min, + 4°C). The resulting pellet was resuspended in buffer 1 and centrifuged a final time (600 g, 5 min, +4°C). After removal of the supernatant, the vessels were then immediately collected in hypotonic buffer (10 mM Tris pH 7.4, 10 mM NaCl, 1.5 mM $MgCl_2$) containing protease inhibitor cocktail and sonicated using a Bioruptor® (Diagenode, Seraing (Ougrée), Belgium).

Preparation of plasma membrane fraction from liver and kidney: Plasma membrane fractions were isolated as described previously with minor modifications (Ohtsuki et al., 2012). Frozen liver (mean and CV, (n=3): 637.6 mg, 4.7% and 623.0 mg, 3.2% for WT and hBCRP mice, respectively) or kidney (mean and CV, (n=3): 578.9 mg, 3.8% and 681.3, 2.8% for WT and

hBCRP mice, respectively) tissues were thawed at +4°C, washed at least twice with isotonic buffer solution 4 (10 mM phosphate buffer pH 7.4, 0.1 M KCl) containing a protease inhibitor cocktail, minced into 1-mm pieces and homogenized by using an Ultraturrax® (IKA®-Werke GmbH & Co. KG, Staufen, Germany) for 5 min at +4°C. The homogenates obtained were centrifuged at 10,800 g for 15 min at +4°C and the supernatants were collected and ultracentrifuged at 100,000 g for 60 min at +4°C. The resulting pellet was resuspended in buffer 5 (20 mM Tris pH 7.4, 0.25 M sucrose, 5.4 mM EDTA) and the suspensions were layered on top of a 38 % sucrose solution and ultracentrifuged at 100,000 g for 30 min at +4°C. The turbid layer at the interface was collected, resuspended in buffer 5, and ultracentrifuged at 100,000 g for 30 min at +4°C. The plasma membrane fraction was obtained from the resulting pellet which was resuspended in buffer 5 containing protease inhibitor cocktail.

Protein digestion: Plasma membrane fractions were digested as described previously without modifications (Hoshi et al., 2013; Uchida et al., 2013). Briefly, 50 µg of proteins were solubilized in denaturing buffer (7 M guanidine hydrochloride, 10 mM EDTA, 500 mM Tris pH 8.5), reduced by DTT and alkylated by iodoacetamide. The alkylated proteins were precipitated with methanol-chloroforme-water, resolubilized in 1.2 M urea, 0.1 M Tris pH 8.5. Samples were first digested using rLysC endoprotease (enzyme:protein ratio = 1:50) during 3 hours at room temperature. Then trypsin (enzyme:protein ratio = 1:100) and 0.05% (W/W) ProteaseMAX were added and samples were incubated at 37°C overnight. The stable isotope-labeled peptide mixture (750 fmol of each labeled peptide) was added in trypsic digest before UHPLC-MS/MS analysis.

Protein Quantification by UHPLC-MS/MS: Na^+/K^+ATPase, and BCRP/Bcrp proteins were quantified by the determination of the peptide concentration using UHPLC-MS/MS in multiplexed selected reaction monitoring (SRM) method. Each peptide analyzed was specific to each protein and was released after protein digestion by trypsin. The selected peptides for

quantification of Na^+/K^+ATPase (AAVPDAVGK) had already been reported by Kamiie et al (Kamiie et al., 2008). One peptide common to human BCRP and mouse Bcrp, SSLLDVLAAR, also selected by Kamiie et al. (Kamiie et al., 2008), was used for quantification. *In silico* criteria, defined by Kamiie et al. (Kamiie et al., 2008), were applied to select specific peptides for human BCRP and mouse Bcrp, which were used for qualitative identification and confirmed the interspecies specificity of the protein. Samples were injected into an Acquity UPLC® system (Waters, Manchester, UK), equipped with an Acquity UPLC BEH® C18 column (Peptide BEH® C18 Column, 300Å, 1.7 µm, 2.1 X 100 mm) supplied by Waters (Guyancourt, France). The mobile phase consisted of mixture of water (formic acid 0.1% (V/V)) and acetonitrile. It was operated with a flow-rate of 0.5 mL/min in gradient mode, at a temperature of 30°C. The total duration of analysis was 30 min. Data were recorded with a Waters Xevo® TQ-S mass spectrometer (Waters, Manchester, UK). Measurements were performed by using positive electrospray ionization (ESI) with ion spray capillary voltage at 2.80 kV. Drying gas temperature was set to 650°C at a flow-rate of 800 L/h. Detection was performed in multiplexed SRM mode using three or four transitions per native or labeled peptide (Supplementary Table 2). Skyline software (MacLean B, et al. Bioinformatics. 2010, 26:966–8) was used for the optimization of the specific transition parameters (i.e; collision energy and peak integration). The area ratios light to labeled peptide were exported from Skyline and quantification was performed from calibration curves by using an *at home* R script.

Sulfasalazine pharmacokinetic and sulfasalazine/Ko143 interaction studies. *In vivo Studies:* All studies performed were approved by the Institutional Animal Care and Use Committee at Genentech, Inc. (South San Francisco, CA). 9-14 week old C57BL/6 WT, $Bcrp^{-/-}$ and hBCRP male mice were used in the studies. Mice were not fasted during the studies. Sulfasalazine was prepared either in 30% Hydroxypropyl-β-cyclodextrin for iv administration (5 g/kg) or as a suspension in 0.5% methylcellulose with 0.2% Tween80 for oral (po) dosing

at 20 mg/kg. Four mice from each strain received the iv dose and 15 µL of blood was taken via tail nick at 0.033, 0.25, 1, 2, 4 and 6 hrs post-dose. Blood was added to 60 µL of EDTA/ water then vortexed and stored at -80ºC until analysis. A crossover study design was used for the po administration. Four mice from each strain were given a dose of 20 mg/kg sulfasalazine and 15 µL of blood was taken via tail nick at 0.25, 0.5, 1, 2, 4 and 6 hrs post-dose. These mice were given a 7-day washout period and in the second part of the study were treated with Ko143 (po, 20 mg/kg) 30 minutes prior to the administration of sulfasalazine (po, 20 mg/kg in 0.5% methylcellulose with 0.2% Tween80). Blood was collected and processed as described for the iv administration. The concentration of sulfasalazine in blood was determined by LC-MS/MS analysis.

LC-MS/MS Analysis: Sulfasalazine blood concentrations were determined by liquid chromatography-tandem mass spectrometry (LC-MS/MS) using a non-validated method. Following protein precipitation with acetonitrile, the supernatant was injected onto a Phenomenex Kinetex PhenylHexyl column (50 × 2 mm, 2.6 µm particle size). A Shimadzu Sil-30AC autosampler linked to a Shimadzu CBM-20A controller with LC-30AD pumps (Shimadzu, Columbia MD), coupled with an ABSciex Qtrap5500 mass spectrometer (Applied Biosystems, Foster City, CA) was used for the LC-MS/MS assay. The aqueous mobile phase was water with 0.1% formic acid (A) and the organic mobile phase was acetonitrile with 0.1% formic acid (B). The gradient was as follows: 5% B for the first 0.3 minutes, increased to 98% B from 0.3 to 0.8min, kept at 98% B until 1.21minutes and decreased to 5% B at 1.22min. The total run time was 1.5 min with a flow rate set at 1.4 ml/min and the ionization was conducted in the positive ion mode using the transition m/z 399 → 381 for sulfasalazine in ESI mode. An internal standard with the transition of 358 → 139 was used. The injection volume was 2 µL. The lower limit of quantitation (LLOQ) of the assay was 0.022 µM for sulfasalzine.

Pharmacokinetic Analysis: Pharmacokinetic parameters were calculated by non-

compartmental methods as described in Gibaldi and Perrier (Gibaldi and Perrier, 1982) using Phoenix™ WinNonlin® Version 6.3 (Pharsight Corporation, Mountain View, CA).

Daidzein in vivo studies. *In vivo study:* All studies performed were approved by the Institutional Animal Care and Use Committee at Janssen R&D (Spring House, PA). Mature C57BL/6 WT, $Bcrp^{-/-}$ and hBCRP male mice were used in the studies. Mice were fed for the duration the study. Daidzein was freshly prepared as a solution in 20% Hydroxypropyl-β-cyclodextrin for iv administration (5 mg/kg). Six mice from each strain received the iv dose via tail vein injection and 30 µL of blood was taken via saphenous vein at 0.083, 0.25, 0.5, 1, 2, 4, 7 and 24 hours post-dose by sparse sampling. Blood was collected into lithium heparin coated tubes and processed to collect 10 µL of plasma which was stored at -80ºC until analysis. After the 24 hour blood collection, a tissue distribution study was conducted using the same mice. Six mice from each strain were dosed with a second iv injection and blood and tissues were collected from two animals at each time point (0.5, 2 and 4 hours post-dose), and blood was processed for analysis as described above. Whole brain was collected from each animal, rinsed and weighed before storing at -80ºC until analysis. The concentration of diadzein in plasma and tissues was determined by LC-MS/MS analysis.

LC-MS/MS Analysis: Daidzein plasma and tissue concentrations were determined by liquid chromatography-tandem mass spectrometry (LC-MS/MS) using a non-validated method. Tissues were homogenized with PBS prior to analysis. Following protein precipitation with acetonitrile, the supernatant was injected onto a Princeton Chromatography C18 column (50 × 2 mm, 5 µm particle size). A HTP PAL Leap autosampler (Leap Technologies, Carrboro NC) linked to a Shimadzu CBM-20A controller with LC-20AD pumps (Shimadzu, Columbia MD), coupled with an ABSciex Qtrap4000 mass spectrometer (Applied Biosystems, Foster City, CA) were used for the LC-MS/MS assay. The aqueous mobile phase was water with 10 mM ammonium formate (A) and the organic mobile phase was acetonitrile (B). The gradient was as follows: 10% B for the first 0.1 minutes, increased to 90% B from 0.1 to 1.25min, kept

at 90% B until 2.00 minutes and decreased to 10% B at 2.25 minutes. The total run time was 3.5 minutes with a flow rate at 0.5 mL/min and the ionization was conducted in positive ion mode using the transition m/z 255 → 91 for diadzein in ESI mode. The internal standard Tolbutamide, with the transition of 272 → 155 was used. The injection volume was 10 µL. The LLOQ of the assay was 10 ng/mL for daidzein in plasma and 5 ng/mL in brain homogenate.

Pharmacokinetic Analysis: Pharmacokinetic parameters were calculated by non-compartmental methods using Phoenix™ WinNonlin® Version 6.3 (Pharsight Corporation, Mountain View, CA).

Genistein in vivo study. *In vivo study:* Genistein was formulated in 30% Captisol (sulfobutyl ether- 7- Beta-cyclodextrin). Eight mice from each strain received an iv dose of 20mg/kg genistein. 10 µL of blood collected via tail vein sampling at 0.08, 0.25, 0.5, 1, 2, 3, 5 and 24h post dose was stabilized with sodium citrate and formic acid. Urine and feces were also collected over this 24h period. With a 7-day washout in between each study, 3 additional arms po 20mg/kg, po 50 mg/kg and iv 20mg/kg were run. The last arm (iv 20mg/kg) included a terminal collection of blood, plasma, brain, liver, kidney and testis at 15 and 90 minutes post dose (n=4 per strain). Samples were stored at -80°C until analysis. The concentration of genistein in blood and tissues was determined by LC-MS/MS analysis.

LC-MS/MS Analysis: Genistein blood, brain, liver, kidney, testes, urine, and feces concentrations were determined by (LC-MS/MS. Blood and urine samples were treated directly with 0.5% formic acid in acetonitrile to effect protein precipitation. Tissue samples were first homogenized with water (1:3 ratio, tissue:water) on a 2000 Geno/Grinder (SPEX, LLC), then an aliquot of the homogenate taken for treatment with 0.5% formic acid in acetonitrile. Following protein precipitation, the supernatants were diluted with water and injected onto a Waters Acquity T3 column (50 x 2.1 mm, 1.7 µm particle size). The LC-MS/MS assay was conducted on a Thermo Transcend LX-2 UPLC running Aria 1.7 software

(Thermo Scientific, Somerset, NJ), coupled to an ABSciex API 5000 mass spectrometer running Analyst 1.6.2 (Applied Biosystems, Foster City, CA). The aqueous mobile phase (A) was water containing 0.1% formic acid, and the organic mobile phase (B) was acetonitrile containing 0.1% formic acid. To resolve the analyte chromatographically, a gradient elution was used as follows: 5% B for the first 0.5 minutes, increased steadily to 95% B over three minutes, maintained at 95% B for 0.2 minutes, then decreased instantaneously to 5% B and held there for 1 minute. The total run time was 4.7 minutes with a flow rate of 0.7 mL/min. To detect the analyte, ESI was used in the negative ion mode. Genistein was monitored with the transition m/z -269 → -133. d4-genistein was used as internal standard and monitored with the transition m/z -273 → -137. The injection volume was 20 µL. The LLOQ of the assay for genistein in blood and urine were 0.0444 µM and 5.25 µM, respectively. The relatively higher LLOQ for urine samples was due to matrix interferences. The LLOQ for the tissues tested were in the ranges of 0.00342 – 11.0 µM.

Pharmacokinetic Analysis: Pharmacokinetic parameters were calculated by noncompartmental methods using Watson LIMS 7.4.1 (Thermo Scientific, Philadelphia, PA).

Rosuvastatin in vivo study. *In vivo study:* Three different study phases were performed with each of the three mouse lines tested (WT, hBCRP, Bcrp$^{-/-}$). As the same animals (n=4/Group) were dosed and sampled at each phase, there was a two weeks recovery period in between. In phase I, a 1 mg/mL rosuvastatin solution was prepared in 2% 1-methyl-2-pyrrolidone (NMP) and 10% Solutol in saline. Animals were iv dosed via a tail vein at 5 mg/kg. In phase II, a 1.5 mg/mL rosuvastatin solution was prepared in 0.5% hydroxypropyl methycellulose (HPMC). Animals (n=4/Group) were po dosed at 15 mg/kg. Following administration in phase I and II, animals were placed in individual metabolism cages for urine and feces (phase II only) collection. Serial blood samples (25µL) were collected via tail snip into a capillary tube. Blood samples were collected at the following times: 0.033, 0.083, 0.167 (iv dose only), 0.25 (po dose only), 0.5, 1, 2, 6 and 24 hours after dosing. Urine and feces were collected over the

24 hour period. In phase III, the animals were dosed iv with a 1 mg/mL rosuvastatin solution prepared in 2% NMP and 10% Solutol in saline. The animals (n=3/Group/time point) were euthanized with CO_2 at 15 minutes and 1 hour after dosing, a sample of blood (25 μL), the liver, the kidney and the brain were collected. Immediately after collection, blood samples were placed into an appropriately labeled matrix tube containing 2.5 μL of 0.1M thenyoltrifluoroacetone (TTFA), 2.5 μL of 0.5M Ammonium acetate and 20 μL of water. The samples were vortex mixed to ensure complete mixing, frozen on dry ice and stored at -70°C or below until analysis. The collected urine samples were treated with 8% Tween20 at 10 uL/100 uL of urine and 0.5M ammonium acetate, pH5.0 at 10 uL/100 uL of urine. The treated urine samples were stored at -70°C or below until analysis. The collected feces were stored at -70°C or below. For homogenization, the feces were thawed on wet ice and pretreated water (treated with 10 uL of 0.1M TTFA and 0.5M ammonium acetate per 100 μL of water) was added to the feces at a volume of 3x the feces weight. The feces were then homogenized using a gentleMACS dissociator (Miltenyi Biotec GmbH, Germany). The homogenate were stored at -70°C or below until analysis. For organ homogenization, the organs were thawed on wet ice and pretreated mouse blood (treated with 10 uL of 0.1M TTFA and 0.5M ammonium acetate per 100 μL of blood) was added to the organs at a volume of 3x the organ weight. The organs were homogenized using a gentleMACS dissociator. The homogenate were stored at -70°C or below until analysis. Individual t-tests with unequal variances were used to analyze the data in most cases although if significance was found, multiple comparisons were done to confirm which groups were different.

LC-MS/MS Analysis: Blood/water, tissues, urine and feces samples were stored in -80°C prior to extraction and analysis. At the day of analysis, blood/water and tissue samples were thawed at ambient conditions and then an aliquot of 25 μL samples were transferred to a 1.4 mL polypropylene Matrix™ tube. Rosuvastatin was extracted from mouse blood/water and tissues

by protein precipitation using a solution of 100 μL, acetonitrile containing an internal standard (IS); 100 ng/mL). Transfer 75μL of the supernatant to clean deep well plate containing 50 μL of water. At the day of analysis, urine and feces samples were thawed at ambient conditions and then an aliquot of 50 μL urine and feces were transferred to an Artic White 96 well polypropylene plate. Rosuvastatin was extracted from urine and feces by liquid-liquid extract (LLE) using a solution of 25 μL, acetonitrile containing an internal standard (IS); 100 ng/mL), 50 μL of 1% formic acid and 1000μL of MtBE. The organic layer is evaporated under a nitrogen stream at approximately 45°C, and the remaining residue is reconstituted with 200 μL of 50%:50% water and acetonitrile. Extracted samples were analyzed by LC-MS/MS using a TurboIonSpray™ interface and multiple reaction monitoring. The analytical column was an ACQUITY UPLC™ HSS T3, 2.1 x 50 mm, with 1.8 μm particle size from Waters Co (Milford, MA, USA). The column temperature was held at 65ºC and the sample compartment was kept at ambient temperature. The Mobile phase A consisted of 0.1% formic acid in water and mobile phase B was acetonitrile with 0.1% formic acid. The initial condition was 30% B until 1.0 min followed by a linear gradient ran from 30% B to 70% B until 1.5 min. The total run time, including sample loading was approximately 1.5 min and the flow rate was maintained at 1.0 mL/min throughout the run and a typical injection volume of 7 μL in a 10 μL loop (partial loop injection mode) was used. A solution of 30% and 70% acetonitrile in water was used as autosampler weak wash and a solution of 40% acetonitrile/40% of IPA/ 20% formic acid in water as strong wash, respectively. An API-4000 mass spectrometer with a TurboIonspray interface (TIS) was operated in the positive ionization mode. The instrument was optimized for rosuvastatin and internal Standard (IS) by infusing a 50 ng/mL solution of 50% mobile phase A and 50% mobile B at 1.0 mL/min through an Agilent pump 1100 series (Palo Alto, CA, USA) directly connected to the mass spectrometer. The MRM transitions of m/z 482 → 258 and m/z 491 → 267 were chosen for

rosuvastatin and IS, respectively. Dwell times of 150 msec were used for both rosuvastatin and its internal standard. The optimized mass spectrometric conditions included the following MS conditions: TIS source temperature, 650ºC; TIS voltage, 5500 V; curtain gas, 30 psi (nitrogen); nebulizer gas (GS1), 50 psi (zero air); turbo gas (GS2), 50 psi (zero air). A collision energy of -45 eV and a declustering potential (DP) of 70 V were used for the analyte and IS. MS data were acquired and processed (integrated) using the proprietary software application Analyst™ (Version 1.6.1, Applied Biosystems/MDS-Sciex, Canada). A calibration plot of analyte/internal standard peak area ratio rosuvastatin concentrations was constructed and a weighted $1/x^2$ linear regression was used. Concentrations of rosuvastatin samples were determined from the appropriate calibration line and used to calculate the bias and precision of the method with an in-house LIMS (Study Management System, SMS2000, and version 2.3, GlaxoSmithKline). SFC data were processed and acquired using MassLynx 4.1 software from Waters Co (Milford, MA, USA). The assay concentration range of 1 to 1000 ng/mL were used for analyzing all the samples.

Topotecan in vivo study. *In vivo study:* hBCRP, Bcrp$^{-/-}$ and C57BL/6 WT mice (8 animals each) were dosed with topotecan dissolved in 5% (w/v) D-Glucose, at a dose of 1 mg/kg iv via the tail vein. Following a 2-week washout period, the same animals were dosed at 1 mg/kg by oral gavage. Blood samples of 10 µl were collected from each animal through microsampling from the saphenous vein at 6 (only iv), 15, and 30 minutes and 1, 2, 4, and 8 hours. 10 µl of each blood sample were immediately added to 30 µl of sterile water in Micronic PP tubes (Micronic, Aston,PA) and stored at -20°C until use. Following another 2-week washout period, the animals were again dosed at 1 mg/kg po. At 15 minutes, or 1 hour post-dosing (4 animals per group), the mice were deeply anesthetized with isoflurane and euthanized; terminal bleeds taken by cardiac puncture, and brains were isolated and stored at -20°C until use.

LC-MS/MS Analysis: Topotecan blood, urine feces and brain concentrations were determined

by LC-MS/MS using a qualified method. Following protein precipitation with acetonitrile, the supernatants were injected onto a Waters HSS T3 column (50 × 2.1 mm, 1.8 µm particle size). A Shimadzu Sil-30ACMP autosampler linked to a Shimadzu CBM-20A controller with LC-30AD pumps (Shimadzu Deutschland, Düsseldorf), coupled with an ABSciex Qtrap5500 mass spectrometer (AB Sciex Germany,Darmstadt) was used for the LC-MS/MS assay. The aqueous mobile phase was water with 0.1 % formic acid (A) and the organic mobile phase was acetonitrile with 0.1 % formic acid (B). The gradient was as follows: 5 % B for the first 0.1 minutes, increased to 95 % B from 0.1 to 0.4 min, kept at 95 % B until 0.9minutes and decreased to 5% B at 0.91 min. The total run time was 1.5 min with a flow rate set at 1.4 ml/min and the ionization was conducted in the positive ion mode using the transition m/z 422.4 → 377.1 for topotecan in ESI mode. As internal standard D6-topotecan was used with the transition of 428.4 → 377.1 was used. The collision energy was 32 V. The injection volume was 10 µL. The lower limit of quantitation (LLOQ) of the assay was 0.9 ng/mL blood for topotecan.

Pharmacokinetic Analysis: Pharmacokinetic parameters were calculated by compartmental analysis using Phoenix WinNonlin 6.3 (Pharsight Corporation, Mountain View, CA).

Positron emission tomography (PET) study. *General:* Tariquidar dimesylate was freshly dissolved prior to each administration in 2.5% (w/v) aqueous (aq.) dextrose solution and injected intravenously (i.v.) at a volume of 4 mL/kg body weight. Ko143 was freshly dissolved prior each application in DMSO and further diluted with a solution of Tween 80, PEG 300 and sterile water (10/25/65, v/v/v) to a final DMSO concentration of 5% (v/v). Formulated Ko143 solution was injected iv into mice at a volume of 4 mL/kg body weight. [^{11}C]Tariquidar was synthetized as described in the literature (Bauer et al., 2010) and formulated in 0.9% aq. saline containing 1% (v/v) Tween 80 to an approximate concentration of 370 MBq/mL. Radiochemical purity, as determined by radio-HPLC was >95%, and specific activity at end of synthesis was > 100 GBq/µmol.

Animals: Female hBCRP and C57BL/6N WT littermates were obtained from Taconic Biosciences GmbH (Cologne, Germany). All animals were housed in groups under individual ventilated cage conditions in polysulfon type III cages. The environmental conditions were: temperature: 22±3°C, humidity: 40% to 70% and a 12-hour light/dark cycle (lights on at 6:00) with free access to standard laboratory rodent diet (ssniff R/M-H, ssniff Spezialdiäten GmbH, Soest, Germany) and tap water. An acclimatization period of at least 1 week was allowed before the animals were used in the experiments. All animal experiments were approved by the national authorities (Amt der Niederösterreichischen Landesregierung) and all study procedures were performed in accordance with the European Communities Council Directive of September 22, 2010 (2010/63/EU). All efforts were made to comply with the 3Rs principle in this study.

Positron Emission Tomography (PET) Imaging: PET imaging was performed at the AIT Austrian Institute of Technology GmbH (Austria). The experimental design was based on previous work (Wanek et al., 2012). In brief, female hBCRP mice (23.3 ± 1.4 g) and WT control mice (23.2 ± 1.5 g) were randomly assigned to 3 study groups consisting of 4-6 mice each. All pretreatment solutions were administered iv. The first group (veh/veh) was pretreated two hours prior start of PET imaging by injection of 2.5% (w/v) aq. dextrose solution. At one hour prior to start of PET scan, mice were additionally pretreated with Ko143 vehicle solution. The second group (TQD/veh) was pretreated two hours prior PET imaging with 12 mg/kg tariquidar solution, followed by Ko143 vehicle solution administered at one hour before start of PET. The last group (TQD/Ko143) received 12 mg/kg tariquidar solution two hours prior PET imaging and additionally 10 mg/kg Ko143 solution at one hour before start of PET. PET imaging was performed using a dedicated small-animal PET scanner (microPET Focus 220, Siemens Medical Solutions, Knoxville, TN, USA) following previously described procedures (Wanek et al., 2012). Dynamic PET scans (0-60 minutes) were recorded after iv injection of 23 ± 13 MBq [^{11}C]tariquidar (containing <0.3 nmol of

unlabelled tariquidar) in a volume of 0.1 mL. After completion of PET data acquisition, blood was withdrawn from the orbital sinus vein and centrifuged to obtain plasma. Animals were sacrificed by cervical dislocation and whole brains were removed. Blood, plasma and brain were measured for radioactivity content in a gamma counter (Perkin-Elmer Instruments, Wellesley, MA, USA). The standard data correction protocol (normalization, decay correction, injection decay correction and attenuation correction) was applied to the acquired PET data which were further sorted into 23 time frames which incrementally increased in time length. Images were reconstructed using Fourier rebinning followed by two-dimensional filtered backprojection. Whole brain regions were manually outlined in the obtained PET images using the image analysis software AMIDE and time-activity curves expressed as standardized uptake value (SUV=((radioactivity per g/injected radioactivity) x body weight) were derived. Brain uptake of [^{11}C]tariquidar was expressed as the brain-to-blood radioactivity concentration ratio ($K_{b,brain}$) derived by dividing the radioactivity concentration in the last frame of the PET image (50-60 minutes) by the blood radioactivity concentration measured at end of PET in the gamma counter.

Metabolite analysis: Blood was centrifuged to obtain plasma and whole brains were removed. Plasma and homogenized brain tissue proteins were precipitated by the addition of acetonitrile (1 µL per 1 µL plasma, 0.2 mL for 0.5 g brain) and samples were spiked with tariquidar reference solution (2.5 mg/mL in 2.5% glucose, 3 µL). The homogenates were vortexed and then centrifuged (12000 × g, 5 min, 21°C). 3 µL of each supernatant (plasma, brain) and diluted [^{11}C]tariquidar solution was spotted on thin-layer chromatography (TLC) plates (silica gel 60F, 20 × 20 cm; Merck, Darmstadt, Germany) which were developed in ethyl acetate/ethanol (6/4, v/v). Detection was performed by placing the TLC plates on multisensitive phosphor screens (Perkin-Elmer Life Sciences, Waltham, MA). The screens were scanned at 300 dpi resolution using a Cyclone® storage phosphor system (Perkin-Elmer Life Sciences).

Statistical analysis: Differences between study groups were analyzed by 1-way analysis of variance (ANOVA) followed by Bonferroni´s multiple comparison test using Prism 6.05 software (La Jolla, CA, USA). The level of significance was set to $P< 0.05$.

Supplemental Methods References

Bauer F, Kuntner C, Bankstahl JP, Wanek T, Bankstahl M, Stanek J, Mairinger S, Dorner B, Loscher W, Muller M, Erker T and Langer O (2010) Synthesis and in vivo evaluation of [11C]tariquidar, a positron emission tomography radiotracer based on a third-generation P-glycoprotein inhibitor. *Bioorg Med Chem* **18**(15):5489-5497.

Dauchy S, Dutheil F, Weaver RJ, Chassoux F, Daumas-Duport C, Couraud PO, Scherrmann JM, De Waziers I and Decleves X (2008) ABC transporters, cytochromes P450 and their main transcription factors: expression at the human blood-brain barrier. *J Neurochem* **107**(6):1518-1528.

Gibaldi M and Perrier D (1982) *Pharmacokinetics*. Marcel Dekker, New York.

Hoshi Y, Uchida Y, Tachikawa M, Inoue T, Ohtsuki S and Terasaki T (2013) Quantitative atlas of blood-brain barrier transporters, receptors, and tight junction proteins in rats and common marmoset. *J Pharm Sci* **102**(9):3343-3355.

Kamiie J, Ohtsuki S, Iwase R, Ohmine K, Katsukura Y, Yanai K, Sekine Y, Uchida Y, Ito S and Terasaki T (2008) Quantitative atlas of membrane transporter proteins: development and application of a highly sensitive simultaneous LC/MS/MS method combined with novel in-silico peptide selection criteria. *Pharm Res* **25**(6):1469-1483.

Ohtsuki S, Schaefer O, Kawakami H, Inoue T, Liehner S, Saito A, Ishiguro N, Kishimoto W, Ludwig-Schwellinger E, Ebner T and Terasaki T (2012) Simultaneous absolute protein quantification of transporters, cytochromes P450, and UDP-glucuronosyltransferases as a novel approach for the characterization of individual human liver: comparison with mRNA levels and activities. *Drug Metab Dispos* **40**(1):83-92.

Scheer N, Balimane P, Hayward MD, Buechel S, Kauselmann G and Wolf CR (2012) Generation and characterization of a novel multidrug resistance protein 2 humanized mouse line. *Drug Metab Dispos* **40**(11):2212-2218.

Uchida Y, Tachikawa M, Obuchi W, Hoshi Y, Tomioka Y, Ohtsuki S and Terasaki T (2013) A study protocol for quantitative targeted absolute proteomics (QTAP) by LC-MS/MS: application for inter-strain differences in protein expression levels of transporters, receptors, claudin-5, and marker proteins at the blood-brain barrier in ddY, FVB, and C57BL/6J mice. *Fluids Barriers CNS* **10**(1):21.

Wanek T, Kuntner C, Bankstahl JP, Mairinger S, Bankstahl M, Stanek J, Sauberer M, Filip T, Erker T, Muller M, Loscher W and Langer O (2012) A novel PET protocol for visualization of breast cancer resistance protein function at the blood-brain barrier. *J Cereb Blood Flow Metab* **32**(11):2002-2011.

Yousif S, Marie-Claire C, Roux F, Scherrmann JM and Decleves X (2007) Expression of drug transporters at the blood-brain barrier using an optimized isolated rat brain microvessel strategy. *Brain Res* **1134**(1):1-11.

Table S1

qRT-PCR analysis of mouse *Bcrp* and human *BCRP* mRNA expression in various tissues of male and female WT, hBCRP and Bcrp$^{-/-}$ mice.

Data were analysed using comparative cycling time methodology, in which fluorescent output, measured as Ct, was directly proportional to input cDNA concentration. Ct values >38 were interpreted as no expression and the corresponding fields are highlighted in dark grey. Ct values 35-38 were considered to be close to the limit of detection and the corresponding fields are highlighted in light grey. ΔCt values were calculated by the subtraction of the Ct value for the internal standard β-actin of the corresponding mouse and tissue from the Ct value for either mouse *Bcrp* or human *BCRP*, respectively. n=3 mice per sex and mouse line.

			Mouse *Bcrp*				Human *BCRP*			
	Mouse line	Sex	Mean Ct	St Dev Ct	Mean ΔCt	St Dev ΔCt	Mean Ct	St Dev Ct	Mean ΔCt	St Dev ΔCt
Liver	WT	MALE	23.7	0.2	4.8	0.1	40.0	0.0	21.0	0.2
	WT	FEM	25.2	0.1	6.2	0.1	40.0	0.0	21.0	0.2
	hBCRP	MALE	40.0	0.0	21.0	0.1	24.9	0.2	5.9	0.2
	hBCRP	FEM	40.0	0.0	20.9	0.2	25.9	0.3	6.8	0.4
	Bcrp$^{-/-}$	MALE	39.4	1.1	20.3	1.1	40.0	0.0	20.9	0.2
	Bcrp$^{-/-}$	FEM	40.0	0.0	20.8	0.3	40.0	0.0	20.8	0.3
Kidney	WT	MALE	20.9	0.1	2.5	0.2	40.0	0.0	21.6	0.2
	WT	FEM	20.9	0.2	2.6	0.1	40.0	0.0	21.7	0.3
	hBCRP	MALE	39.2	1.4	21.0	1.2	22.4	0.3	4.2	0.1
	hBCRP	FEM	39.2	1.4	21.2	1.0	22.3	0.3	4.3	0.1
	Bcrp$^{-/-}$	MALE	40.0	0.0	21.6	0.2	40.0	0.0	21.6	0.2
	Bcrp$^{-/-}$	FEM	40.0	0.0	22.1	0.2	40.0	0.0	22.1	0.2
Brain	WT	MALE	25.0	0.1	7.3	0.1	38.3	2.3	20.6	2.3
	WT	FEM	25.1	0.1	7.5	0.2	40.0	0.0	22.5	0.2
	hBCRP	MALE	40.0	0.0	22.2	0.2	25.5	0.3	7.7	0.1
	hBCRP	FEM	38.8	1.1	21.2	0.9	25.4	0.5	7.8	0.3
	Bcrp$^{-/-}$	MALE	40.0	0.0	22.0	0.3	40.0	0.0	22.0	0.3
	Bcrp$^{-/-}$	FEM	38.4	2.8	20.5	2.9	38.5	2.6	20.6	2.5

Duodenum	WT	MALE	22.7	0.1	7.1	0.0	40.0	0.0	24.5	0.1
	WT	FEM	22.5	0.3	6.5	0.2	40.0	0.0	24.1	0.2
	hBCRP	MALE	36.9	5.3	21.1	5.3	23.5	0.2	7.7	0.1
	hBCRP	FEM	40.0	0.0	24.1	0.1	23.5	0.3	7.6	0.3
	Bcrp$^{-/-}$	MALE	40.0	0.0	24.1	0.4	40.0	0.0	24.1	0.4
	Bcrp$^{-/-}$	FEM	40.0	0.0	24.1	0.3	40.0	0.0	24.1	0.3
Jejunum	WT	MALE	22.7	0.3	7.3	0.3	40.0	0.0	24.6	0.5
	WT	FEM	23.0	0.4	7.2	0.2	40.0	0.0	24.3	0.2
	hBCRP	MALE	40.0	0.0	24.5	0.2	23.6	0.3	8.1	0.1
	hBCRP	FEM	39.0	1.8	23.4	1.7	23.6	0.3	8.0	0.1
	Bcrp$^{-/-}$	MALE	40.0	0.0	25.5	0.5	40.0	0.0	25.2	0.5
	Bcrp$^{-/-}$	FEM	40.0	0.0	24.7	0.2	40.0	0.0	24.7	0.2
Ileuum	WT	MALE	21.6	0.4	6.3	0.4	40.0	0.0	24.7	0.2
	WT	FEM	20.9	0.2	5.6	0.2	40.0	0.0	24.6	0.3
	hBCRP	MALE	40.0	0.0	24.8	0.3	23.3	0.6	8.1	0.3
	hBCRP	FEM	40.0	0.0	24.5	0.3	23.1	0.4	7.6	0.5
	Bcrp$^{-/-}$	MALE	39.4	1.0	24.1	0.9	40.0	0.0	24.7	0.2
	Bcrp$^{-/-}$	FEM	39.4	1.1	23.8	1.2	40.0	0.0	24.5	0.4
Colon	WT	MALE	22.9	0.3	6.8	0.2	40.0	0.0	23.9	0.2
	WT	FEM	23.1	0.3	6.5	0.0	40.0	0.0	23.4	0.3
	hBCRP	MALE	40.0	0.0	23.8	0.2	24.0	0.1	7.7	0.3
	hBCRP	FEM	40.0	0.0	23.8	0.2	23.9	0.1	7.7	0.2
	Bcrp$^{-/-}$	MALE	38.1	3.3	21.6	3.1	40.0	0.0	23.5	0.9
	Bcrp$^{-/-}$	FEM	39.1	0.8	22.6	0.9	40.0	0.0	23.5	0.2
Heart	WT	MALE	26.4	0.2	6.1	0.2	40.0	0.0	19.7	0.3
	WT	FEM	26.6	0.8	6.5	0.2	40.0	0.0	19.9	0.7
	hBCRP	MALE	38.9	1.9	19.2	1.7	27.4	0.4	7.6	0.2
	hBCRP	FEM	40.0	0.0	19.9	0.3	28.1	0.3	8.1	0.3
	Bcrp$^{-/-}$	MALE	40.0	0.0	19.8	0.3	40.0	0.0	19.8	0.3
	Bcrp$^{-/-}$	FEM	38.4	2.7	18.1	2.6	40.0	0.0	19.7	0.2
Lung	WT	MALE	24.8	0.1	8.3	0.3	40.0	0.0	23.4	0.1
	WT	FEM	25.7	0.8	8.7	0.3	40.0	0.0	23.0	0.5
	hBCRP	MALE	40.0	0.0	23.5	0.2	26.1	0.1	9.5	0.3
	hBCRP	FEM	40.0	0.0	23.3	0.0	26.7	0.2	10.0	0.2
	Bcrp$^{-/-}$	MALE	40.0	0.0	23.3	0.2	40.0	0.0	23.3	0.2
	Bcrp$^{-/-}$	FEM	38.3	3.0	21.4	2.9	40.0	0.0	23.1	0.0
Testis	WT	MALE	23.0	0.6	5.5	0.2	40.0	0.0	22.5	0.4
	hBCRP	MALE	39.1	1.6	21.5	1.6	24.9	0.2	7.3	0.1
	Bcrp$^{-/-}$	MALE	39.8	0.3	22.1	0.3	39.3	1.3	21.5	1.3

Table S2

Target peptides and selected ions used in the UHPLC-MS/MS multiplexed SRM method analysis.

Protein	UniProt Accession	Peptide Sequence	Isotope Type	Precursor M/z	Precursor Charge	Product M/z	Fragment Ion	Product Charge
Bcrp / BCRP	Q7TMS5 / Q9UNQ0	SSLLDVLAAR	light	522.8	2	757.5	y7	1
					2	644.4	y6	1
					2	529.3	y5	1
					2	430.3	y4	1
		SSLLDVLA[+4]AR	heavy	524.8	2	761.5	y7	1
					2	648.4	y6	1
					2	533.4	y5	1
					2	434.3	y4	1
Na+/K+ ATPAse	P05023	AAVPDAVGK	light	414.2	2	756.4	y8	1
					2	685.4	y7	1
					2	586.3	y6	1
					2	489.3	y5	1
		AAVPDAV[+6]GK	heavy	417.2	2	762.4	y8	1
					2	691.4	y7	1
					2	592.3	y6	1
					2	495.3	y5	1

Table S3

Fold changes in gene expression in liver of Bcrp$^{-/-}$ and hBCRP mice compared to WT controls. Only changes > 2 fold and $p<0.05$ are shown. Increased or decreased gene expression is shown as positive or negative values, respectively.

Fold change	p-value	Gene symbol	Gene name
Bcrp-/- versus WT mice			
17.5996	0.0059	Moxd1	monooxygenase, DBH-like 1
8.5719	0.0227	Lcn2	lipocalin 2
4.9139	0.0392	Orm2	orosomucoid 2
4.7255	0.0225	Mt2	metallothionein 2
4.2179	0.0216	Saa3	serum amyloid A 3
2.8737	0.0202	Prtn3	proteinase 3
2.6667	0.0158	S100a8	S100 calcium binding protein A8 (calgranulin A)
2.4048	0.0265	Dnajc12	DnaJ (Hsp40) homolog, subfamily C, member 12
2.3714	0.0183	Atp11a	ATPase, class VI, type 11A
2.1813	0.0152	S100a9	S100 calcium binding protein A9 (calgranulin B)
2.1263	0.0273	Slc3a1	solute carrier family 3, member 1
2.0469	0.049	Cxcl14	chemokine (C-X-C motif) ligand 14
2.006	0.0394	Slc41a2	solute carrier family 41, member 2
-2.0604	0.0175	Unknown	Unknown
-2.105	0.0006	Prlr	prolactin receptor
-2.1326	0.0045	D0H4S114	DNA segment, human D4S114
-2.1941	0.0064	D0H4S114	DNA segment, human D4S114
-2.2845	0.0445	Socs2	suppressor of cytokine signaling 2
-2.5127	0.0118	Cyp2b10	cytochrome P450, family 2, subfamily b, polypeptide 10
-2.8891	0.0002	Mid1	midline 1
-3.0062	0.0105	Cyp2b10	cytochrome P450, family 2, subfamily b, polypeptide 10
-3.1686	0.0005	Aqp4	aquaporin 4
-3.379	0.0007	Hsd17b6	hydroxysteroid (17-beta) dehydrogenase 6
-87.2417	4.94E-14	Abcg2	ATP-binding cassette, sub-family G (WHITE), member 2
hBCRP versus WT mice			
8.699	0.0244	Moxd1	monooxygenase, DBH-like 1
2.551	0.0085	Serpine2	serine (or cysteine) peptidase inhibitor, clade E, member 2
-2.635	0.0003	Tmem223	transmembrane protein 223
-77.9808	6.21E-14	Abcg2	ATP-binding cassette, sub-family G (WHITE), member 2

Table S4A

Pharmacokinetic parameters after iv (5 mg/kg) and po (20 mg/kg) administrations of sulfasalazine to C57BL/6 WT, $Bcrp^{-/-}$ and hBCRP mice (values reported as mean ± SD; n=4 mice) in the absence or presence of the BCRP inhibitor Ko143 (20 mg/kg, po). Parameters calculated using blood concentrations up to 2 hours (iv) or 1 hour (po).

		5 mg/kg iv Administration		**20 mg/kg po Administration**	
	Mouse Line	CL (ml/min/kg)	AUC_{0-2} (µM*hr)	AUC_{0-1} (µM*hr)	C_{max} (µM)
No inhibitor	C57BL/6 WT	22.8 ± 4.6[a]	9.40 ± 1.91[a]	0.14 ± 0.08[a]	0.25 ± 0.13[a]
	hBCRP	8.49 ± 2.87[a]	25.0 ± 2.9[a]	0.65 ± 0.12[a]	0.92 ± 0.24[a]
	$Bcrp^{-/-}$	2.71 ± 0.22	77.9 ± 6.1	16.4 ± 5.5	26.6 ± 9.5
+ Ko143	C57BL/6 WT	--	--	3.61 ± 1.50[b]	5.36 ± 1.98[b]
	hBCRP	--	--	4.19 ± 1.03[b]	6.64 ± 1.95[b]
	$Bcrp1^{-/-}$	--	--	12.7 ± 0.9	20.5 ± 3.5

[a] Significantly different from $Bcrp^{-/-}$ mice ($p<0.05$).

[b] Significantly different from control study (same mouse line, no inhibitor; $p<0.05$).

AUC_{0-2} (or AUC_{0-1}): Area under the blood concentration-time curve from time 0 to the 2-hour (or 1-hour) concentration.

CL: Blood clearance calculated using AUC_{0-2}.

Table S4B

Pharmacokinetic parameters after iv (5 mg/kg) and po (20 mg/kg) administrations of sulfasalazine to C57BL/6 WT, Bcrp$^{-/-}$ and hBCRP mice (values reported as mean ± SD; n=4 mice) in the absence or presence of the BCRP inhibitor Ko143 (20 mg/kg, po).

		5 mg/kg iv Administration		**20 mg/kg po Administration**	
	Mouse Line	CL (ml/min/kg)	$AUC_{0\text{-last}}$ (µM*hr)	$AUC_{0\text{-last}}$ (µM*hr)	C_{max} (µM)
No inhibitor	C57BL/6 WT	22.8 ± 4.6[a]	9.40 ± 1.91[a]	0.14 ± 0.08[a]	0.25 ± 0.13[a]
	hBCRP	6.63 ± 0.56[a]	30.0 ± 1.8[a]	1.83 ± 0.86[a]	1.29 ± 1.19[a]
	Bcrp$^{-/-}$	0.83 ± 0.07	156 ± 12	145 ± 25	33.0 ± 5.2
+ Ko143	C57BL/6 WT	--	--	6.38 ± 2.12[b]	5.36 ± 1.98[b]
	hBCRP	--	--	9.79 ± 5.53[b]	6.64 ± 1.95[b]
	Bcrp1$^{-/-}$	--	--	120 ± 27	26.9 ± 5.6

[a] Significantly different from Bcrp$^{-/-}$ mice ($p<0.05$).

[b] Significantly different from control study (same mouse line, no inhibitor; $p<0.05$).

$AUC_{0\text{-last}}$: Area under the blood concentration-time curve from time 0 to the last measurable concentration.

Table S5

Blood PK parameters after 20 mg/kg iv, 20 mg/kg oral or 50 mg/kg oral administration of genistein to male C57BL/6 WT, hBCRP and Bcrp$^{-/-}$ mice (n=8 for each line).

20 mg/kg iv administration			
Mouse line	**$AUC_{0\text{-}24hrs}$ (µM*hr)**	**CL (mL/min/kg)**	**Vd_{ss} (L/kg)**
C57BL/6 WT	*22.46 ± 9.56	*60.51 ± 18.05	3.46 ± 4.15
hBCRP	52.0 ± 38.0	45.2 ± 37.1	*2.4 ± 3.3
Bcrp$^{-/-}$	48.38 ± 15.12	25.67 ± 8.07	8.09 ± 5.00
20 mg/kg po administration			
Mouse line	**$AUC_{0\text{-}6hrs}$ (µM*hr)**	**C_{max} (µM)**	**T_{max} (hr)**
C57BL/6 WT	*1.54 ± 0.41	2.40 ± 0.64	0.17 ± 0.00
hBCRP	*2.06 ± 0.40	4.03 ± 0.85	0.17 ± 0.00
Bcrp$^{-/-}$	3.13 ± 1.70	3.14 ± 1.35	0.17 ± 0.00
50 mg/kg po administration			
Mouse line	**$AUC_{0\text{-}24hrs}$ (µM*hr)**	**C_{max} (µM)**	**T_{max} (hr)**
C57BL/6 WT	*4.92 ± 1.16	9.09 ± 2.82	0.17 ± 0.00
hBCRP	*6.90 ± 2.20	9.33 ± 3.01	0.17 ± 0.00
Bcrp$^{-/-}$	10.61 ± 2.67	8.53 ± 3.38	0.17 ± 0.00

*: $P<0.05$ significantly different from Bcrp$^{-/-}$ mice; AUC: Area under the concentration time curve; CL: Clearance; Vd_{ss}: Volume of distribution at steady state; C_{max}: Peak concentration; T_{max}: Time to peak concentration

Table S6

Blood PK parameters after 6.1 mg/kg iv or 13.7 mg/kg oral administration of rosuvastatin to male C57BL/6 WT, hBCRP and $Bcrp^{-/-}$ mice (n=4 for each line).

6.1 mg/kg iv administration		
Mouse line	**$AUC_{0\text{-}24hrs}$ (µg*h/ml)**	**C_{max} (µg/ml)**
C57BL/6 WT	1.75 ± 0.20*	15.0 ± 2.3*
hBCRP	2.02 ± 0.50*	15.1 ± 5.0*
$Bcrp^{-/-}$	7.33 ± 5.01	25.1 ± 8.9
13.7 mg/kg po administration		
Mouse line	**$AUC_{0\text{-}24hrs}$ (µg*h/ml)**	**C_{max} (µg/ml)**
C57BL/6 WT	0.13 ± 0.09*	0.032 ± 0.010*
hBCRP	0.21 ± 0.02*	0.054 ± 0.003*
$Bcrp^{-/-}$	0.41 ± 0.08	0.218 ± 0.040

*: $P<0.05$ significantly different from $Bcrp^{-/-}$ mice; AUC: Area under the concentration time curve; C_{max}: Peak concentration

Table S7

Percent recovery of parent compound in feces and urine after 6.1 mg/kg iv and in urine after 13.7 mg/kg oral administration of rosuvastatin to male C57BL/6 WT, hBCRP and Bcrp$^{-/-}$ mice (n=4 for each line).

	6.1 mg/kg iv		**13.7 mg/kg po**
Mouse line	**Feces**	**Urine**	**Urine**
C57BL/6 WT	51.8 ± 17.2*	0.177 ± 0.168	0.253 ± 0.174
hBCRP	12.2 ± 8.1†	0.091 ± 0.080	0.129 ± 0.090
Bcrp$^{-/-}$	3.1 ± 1.4	0.004 ± 0.004	0.052 ± 0.044

*: P<0.05 significantly different from Bcrp$^{-/-}$ mice

† : P<0.05, significantly different from C57BL/6 WT mice

Table S8

Blood PK parameters after 1 mg/kg iv or oral administration of topotecan to male C57BL/6 WT, hBCRP and Bcrp$^{-/-}$ mice (n=8 for WT iv, Bcrp$^{-/-}$ iv and po and hBCRP iv and po; n=7 for WT po)

1 mg/kg iv administration		
Mouse line	**AUC_{0-8h} (ng*h/ml)**	**CL (L/h/kg)**
C57BL/6 WT	356.5± 18.8***	2.08 ± 0.50***
hBCRP	559.1 ± 39.3***	1.46 ± 0.29
Bcrp$^{-/-}$	743.6 ± 22.9	1.32 ± 0.08
1 mg/kg po administration		
Mouse line	**AUC_{0-4h} (ng*h/ml)**	**C_{max} (ng/ml)**
C57BL/6 WT	35.6 ± 5.2***	17.8 ± 2.4***
hBCRP	144.5 ± 15.2***	57.5 ± 22.7***
Bcrp$^{-/-}$	217.3 ± 21.6	99.4 ± 12.4

*=P<0.05 and ***=P<0.001 significantly different from Bcrp$^{-/-}$ mice; AUC: Area under the concentration time curve; CL: Clearance; C_{max}: Peak concentration